Time-periodic Driving of Nuclear Reactions by Intrinsic Localized Modes Arising in Hydrogenated Metals

Vladimir Dubinko[1], Denis Laptev[2], Klee Irwin[3]

- [1]NSC Kharkov Institute of Physics and Technology, Ukraine
- [2]B. Verkin Institute for Low Temperature Physics and Engineering, Ukraine
- [3]Quantum Gravity Research, USA

Outline

- Localized Anharmonic Vibrations: history and the state of the art
- LAV role in **chemical** and **nuclear** catalysis
- MD simulations in crystals of NiH and Pd nanoclusters at finite temperatures

Energy localization in anharmonic lattices

In the summer of 1953 Enrico Fermi, John Pasta, Stanislaw Ulam, and Mary Tsingou conducted numerical experiments (i.e. computer simulations) of a vibrating string that included a non-linear term (quadratic in one test, cubic in another, and a piecewise linear approximation to a cubic in a third). They found that the behavior of the system was quite different from what intuition would have led them to expect. Fermi thought that after many iterations, the system would exhibit thermalization, an ergodic behavior in which the influence of the initial modes of vibration fade and the system becomes more or less random with all modes excited more or less equally. Instead, the system exhibited a very complicated quasi-periodic behavior. They published their results in a Los Alamos technical report in 1955.

The **FPU paradox** was important both in showing the complexity of nonlinear system behavior and the value of computer simulation in analyzing complex systems.

Localized Anharmonic Vibrations (LAVs)
A. Ovchinnikov (1969)

Two coupled anharmonic oscillators

$$\ddot{x}_1 + \omega_0^2 x_1 + \varepsilon\lambda x_1^3 = \varepsilon\beta x_2$$
$$\ddot{x}_2 + \omega_0^2 x_2 + \varepsilon\lambda x_2^3 = \varepsilon\beta x_1$$

$$\tau = \frac{\omega_0}{\varepsilon\beta}\int_0^{\pi/2} \frac{d\eta}{\sqrt{1-\left(\frac{3A_0\lambda}{4\beta}\right)^2 \sin^2\eta}}$$

Localization condition

$$A_0 > \frac{4\beta}{3\lambda} \Rightarrow \tau \to \infty$$

Phase diagram

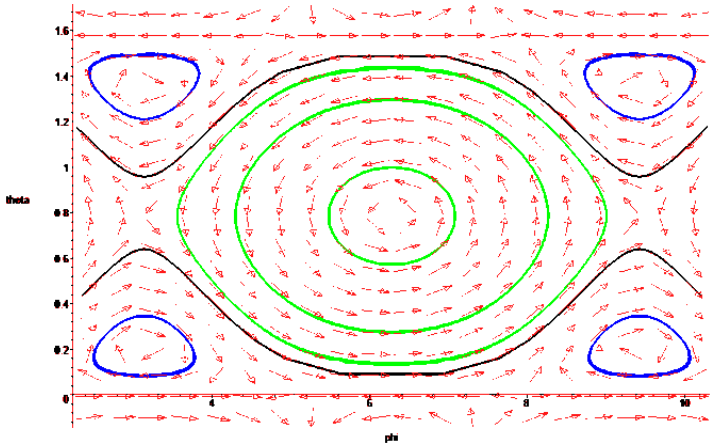

LAV examples:

- ILM/DBs in periodic crystals
- LAVs in disordered systems
- Phasons in quasicrystals
- Calthrate guest-host systems
- Vibrations of ‘magic clusters’
- etc

ILMs in metals Hizhnyakov et al (2011)

PREDICTION OF HIGH-FREQUENCY INTRINSIC . . .

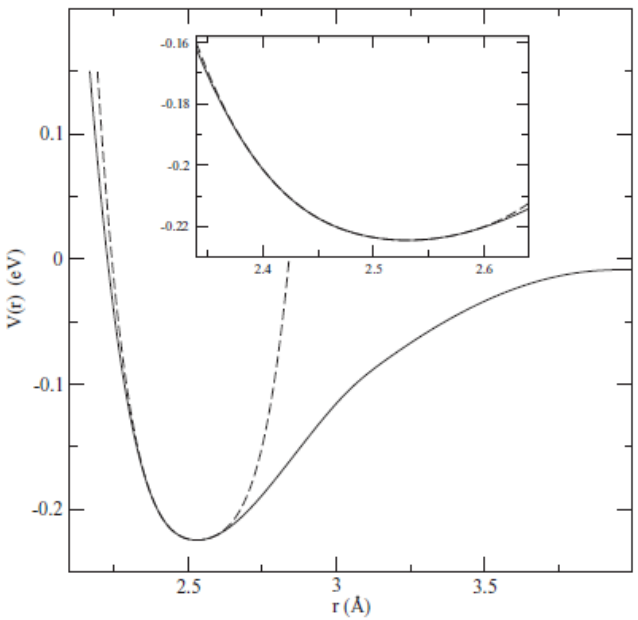

FIG. 1. The pair potential $V(r)$ of Ni (solid line) and its approximation by the fourth-order polynomial (dashed line). The inset shows an expanded view.

The distance between the nearest atoms in Ni at room temperature is $r_0 = 2.49$ Å and longitudinal sound velocity is $v_l = 5266$ m/s. These values give $\tilde{K}_2 = 2.75$ eV/Å^2 (as expected, $\tilde{K}_2 > K_2$) and $\tilde{\kappa} \approx 1.2$. The distance r_0 increases

HAAS, HIZHNYAKOV, SHELKAN, KLOPOV, AND SIEVERS

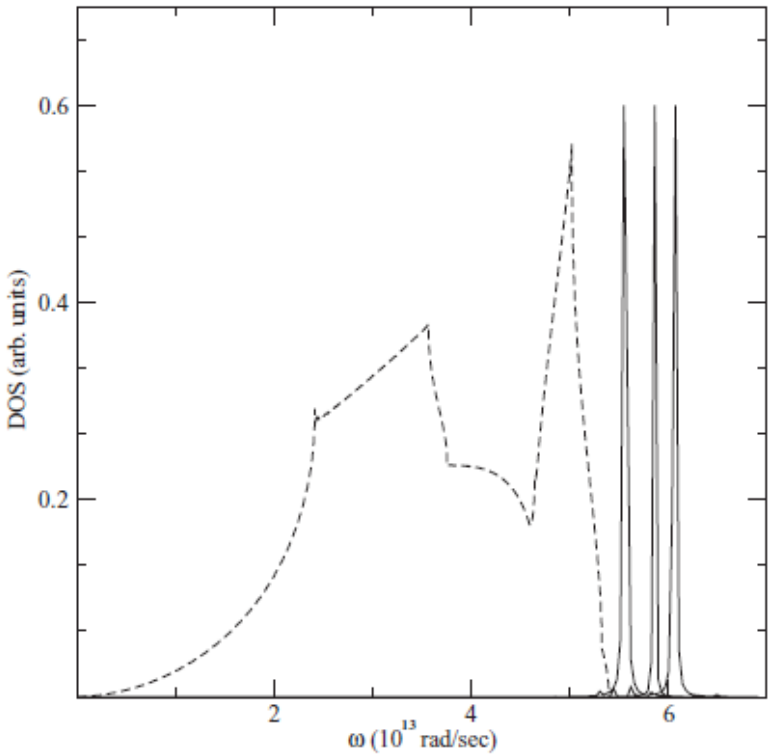

FIG. 2. Phonon density of states and three ILM spectral signatures for Ni. Phonon spectrum (dashed line) and spectrographs (solid line) of the different ILM's: The frequencies are 5.58, 5.86, and 6.07 (10^{13} rad/s) and the amplitudes of vibrations of the central bond are 0.18, 0.31, and 0.42 Å.

Standing DB in bcc Fe: d_0=0.3 Å

D.Terentyev, V. Dubinko, A. Dubinko (2013)

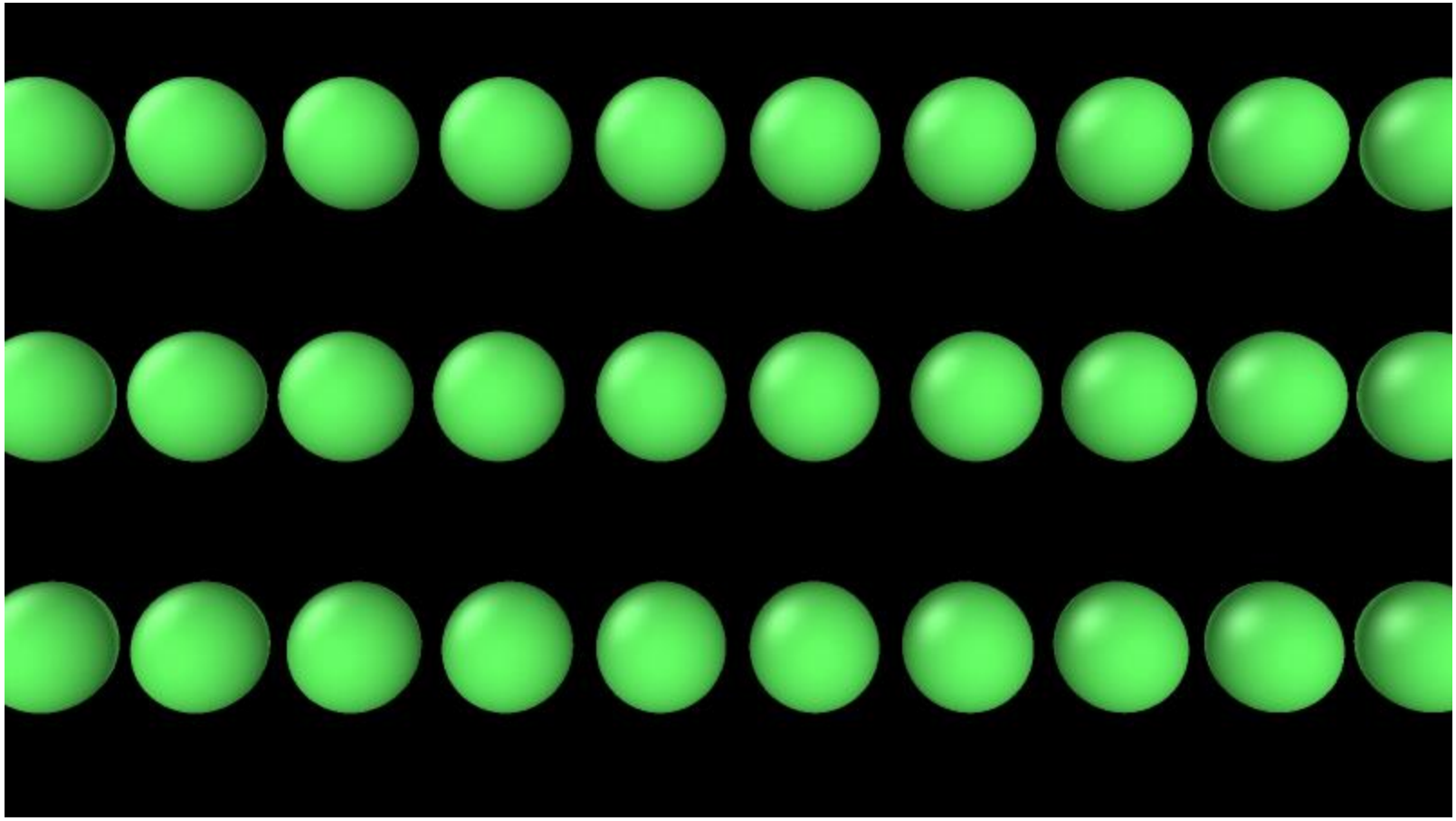

DB along [111] direction in bcc Fe at T=0K

Modelling Simul. Mater. Sci. Eng. **23** (2015) 085007 D A Terentyev *et al*

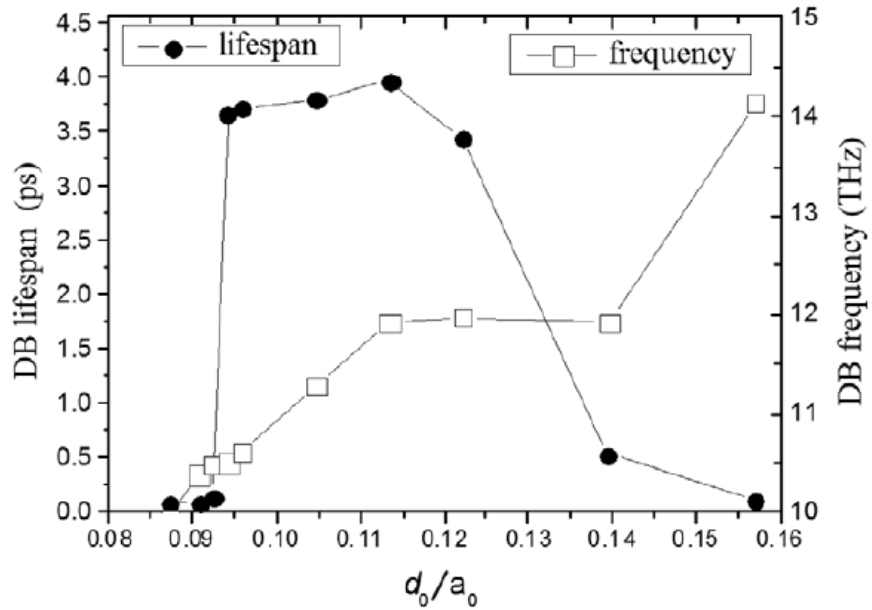

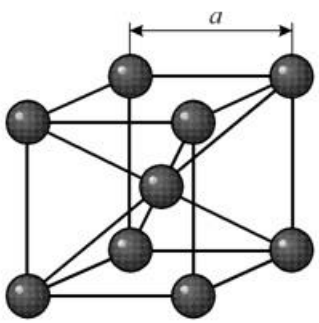

Figure 1. Lifespan and frequency of standing DB as the function of the relative initial displacement d_0/a_0 for the IAP derived in [28].

Initial conditions:

$$x_{n-2} = +0.2 \quad x_{n-1} = -0.2 \quad x_n = +0.4 \quad x_{n+1} = -0.4 \quad x_{n+2} = +0.2 \quad x_{n+3} = -0.2$$

Boundary conditions: periodic

It is seen from the visualization, that the LAV has been generated from the initial anti-phase displacements of 6 atoms.

Moving DB in bcc Fe: d_0=0.4 Å, E= 0.3 eV

D.Terentyev, V. Dubinko, A. Dubinko (2013)

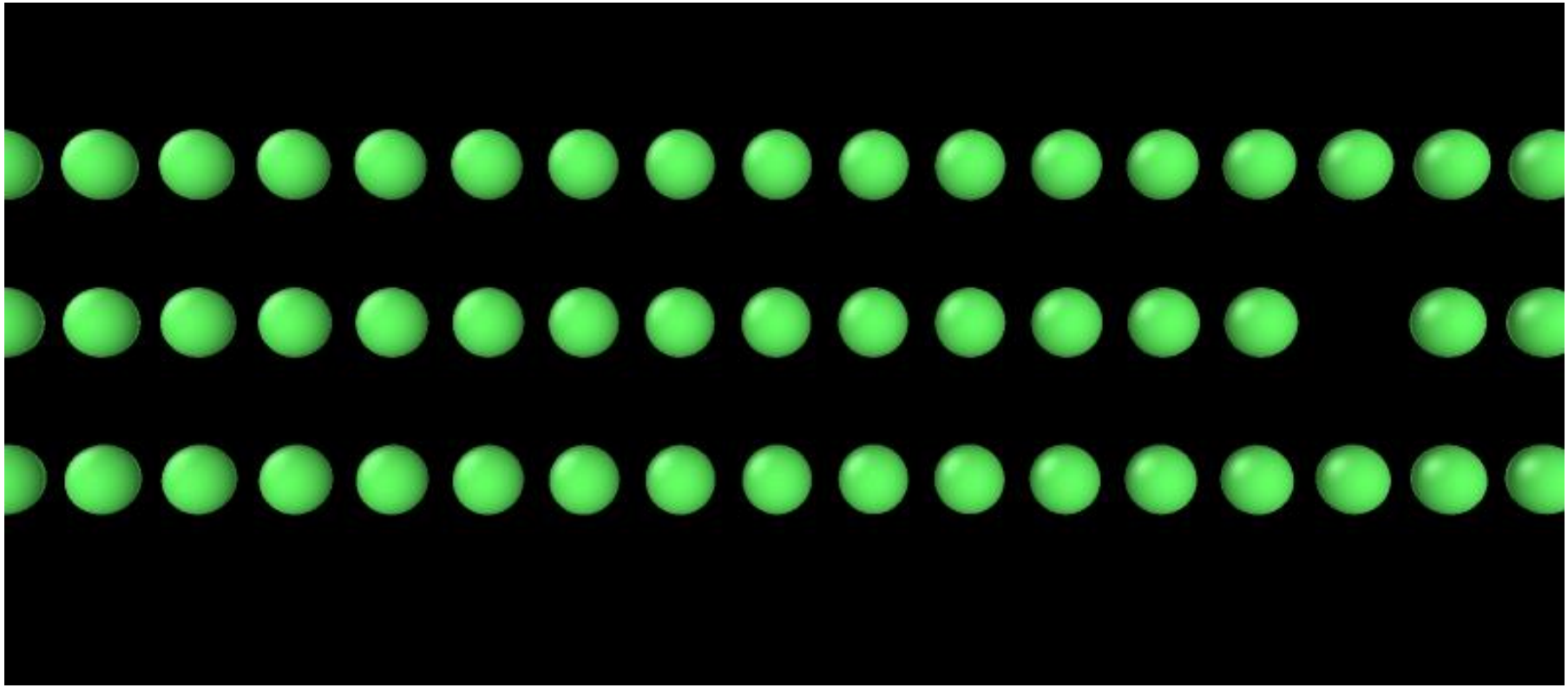

DB in bulk Pd 3D lattice

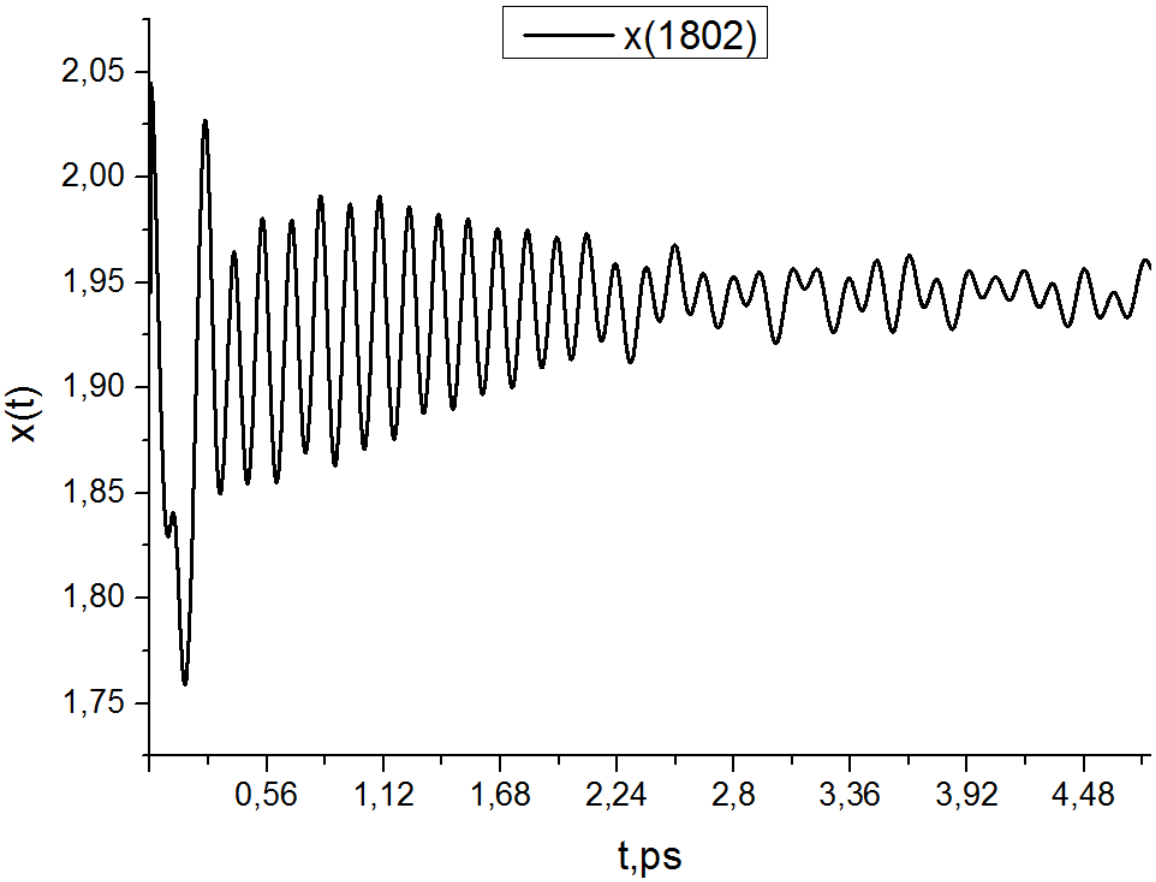

LAV Time Period= 0.1292 ps
LAV frequency = 7.7399 THz

The DB frequency lies above the phonon vibration spectrum

Module of velocity of DB (#1100) and lattice (#1095) atom in fcc Pd lattice

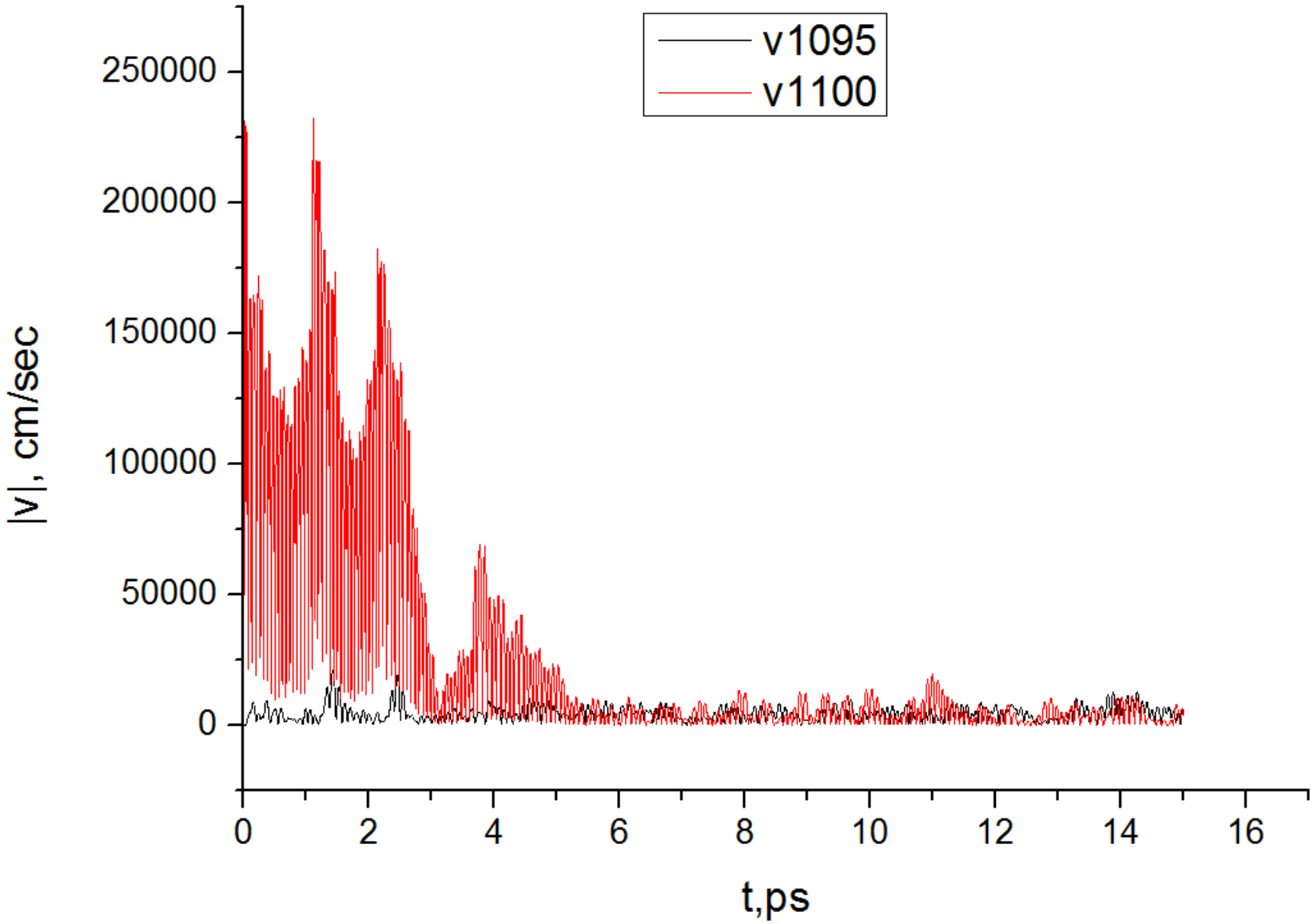

Effective ‘temperature’ of DB (#1100) and lattice (#1095) atom in fcc Pd lattice

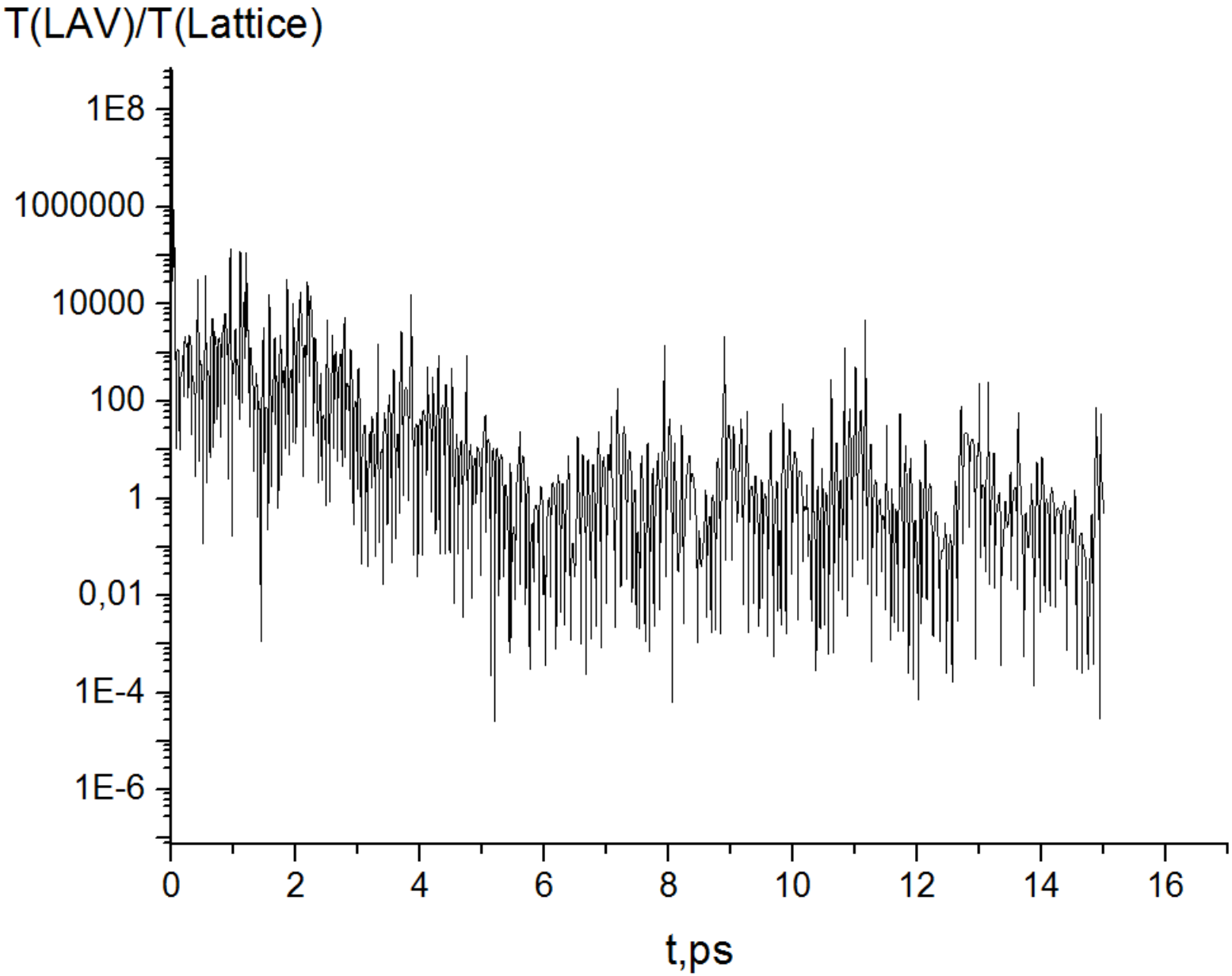

Gap DBs in NaCl type lattices, Dmitriev et al (2010)

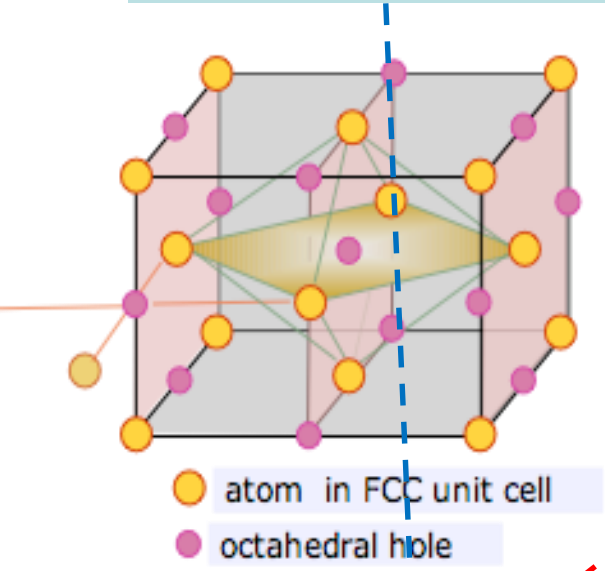

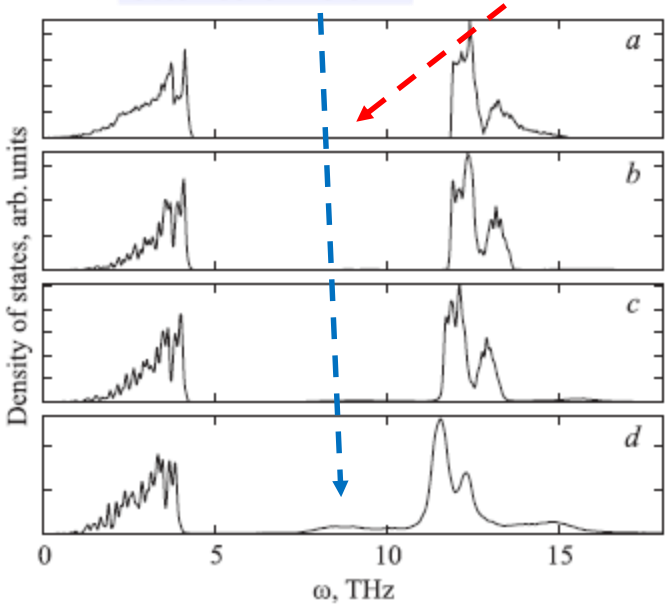

NaCl-type $M_H / M_L = 10$ at temperatures
T = (a) 0, (b) 155, (c) 310, and (d) 620 K

Phonon Gap

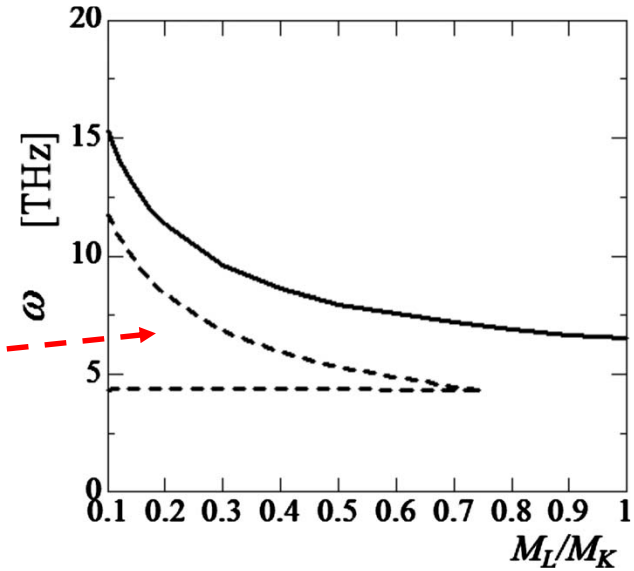

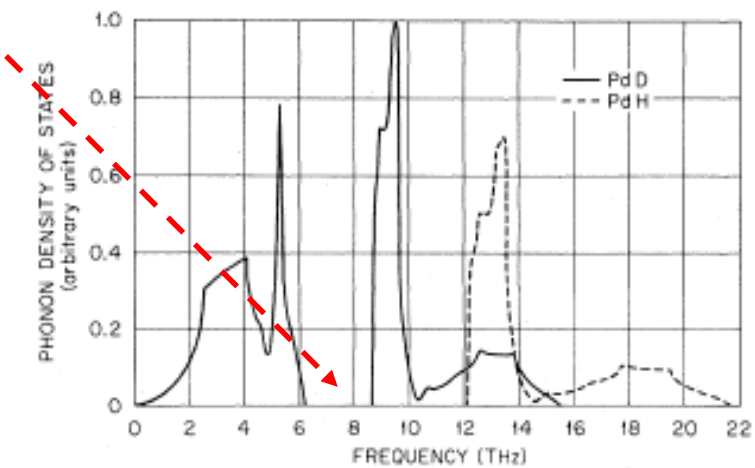

DOS for $\mathbf{PdD_{0.63}}$ and $\mathbf{PdH_{0.63}}$: $M_H / M_L = 50; 100$
D pressure of 5 GPa and T=600 K

MD modeling of gap DBs in diatomic crystals at elevated temperatures

Hizhnyakov et al (2002), Dmitriev et al (2010)

$$K^*_{B,n}/\bar{K} \approx 5.1$$

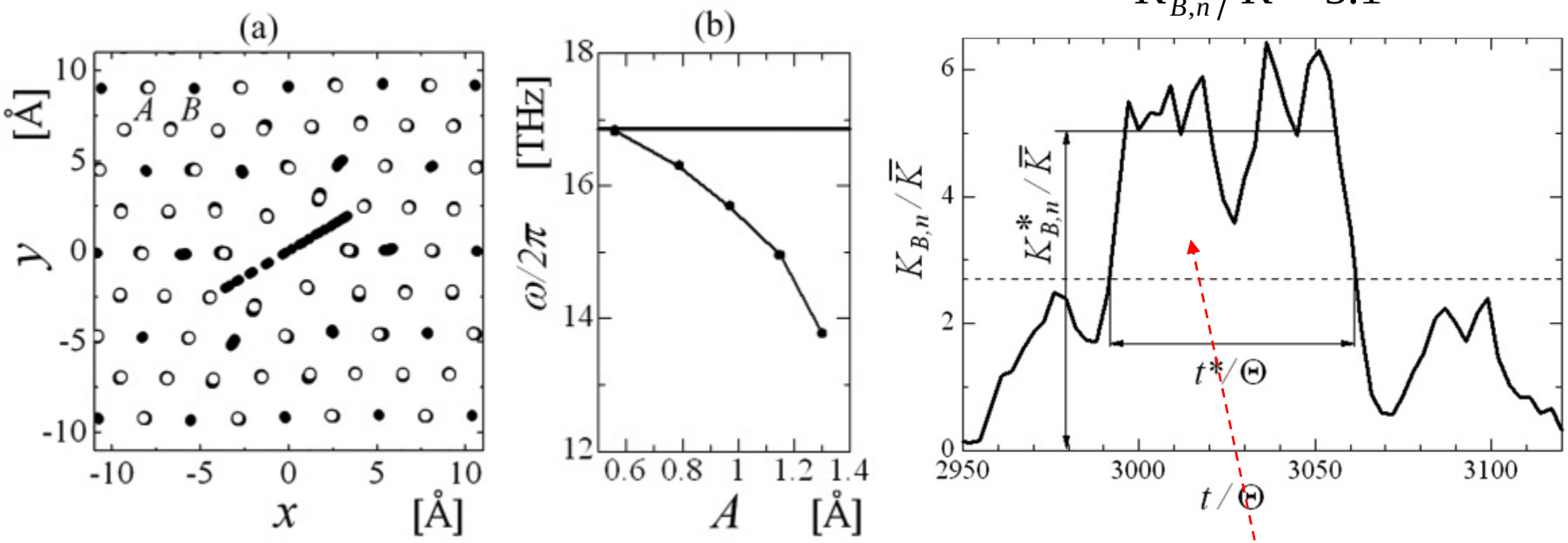

A_3B type crystals $M_H/M_L = 10$

$$t^*/\Theta \approx 70 \quad \bar{K} = 0.1eV \geq 1000K$$

In NaI and KI crystals Hizhnyakov et al has shown that DB amplitudes along <111> directions can be as high as 1 Å, and $t^*/\Theta \sim 10^4$

Lifetime and concentration of ***high-energy light atoms*** increase exponentially with increasing T

MD modeling of gap DBs in diatomic crystals

A_3B type crystals, Kistanov, Dmitriev (2014),

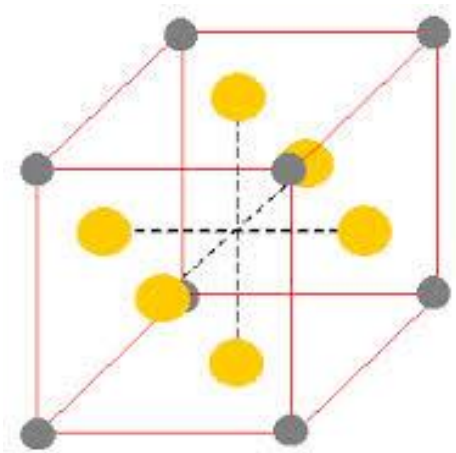

A_3B compound based on fcc lattice with Morse interatomic potentials. Grey atoms are **50 times lighter** than yellow (similar to the PdD crystal).

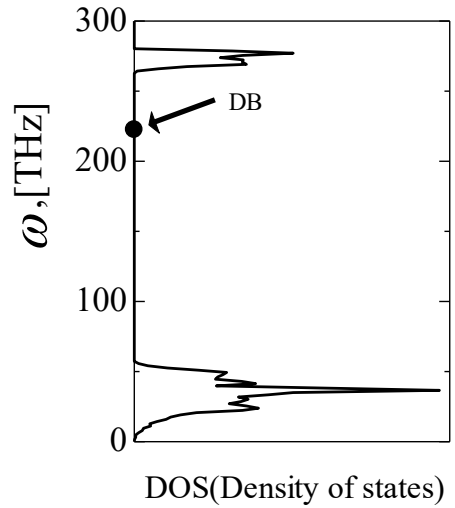

DOE of a A_3B compound with $M_H / M_L = 50$

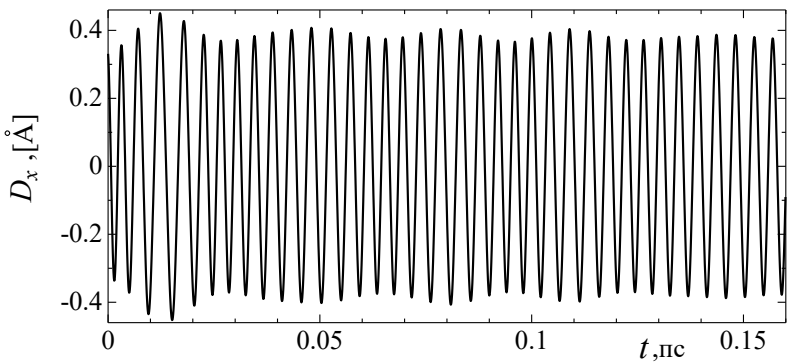

DB is localized on a single light atom vibrating along <100> direction with the frequency of 227 THz, which is **inside the phonon gap**. Shown is the x-displacement of the light atom as the function of time. DB has very large amplitude of 0.4 angstrom, which should be compared to the lattice parameter a=1.35 angstrom

LAV effect (1): peiodic in time modulation of the potential barrier height

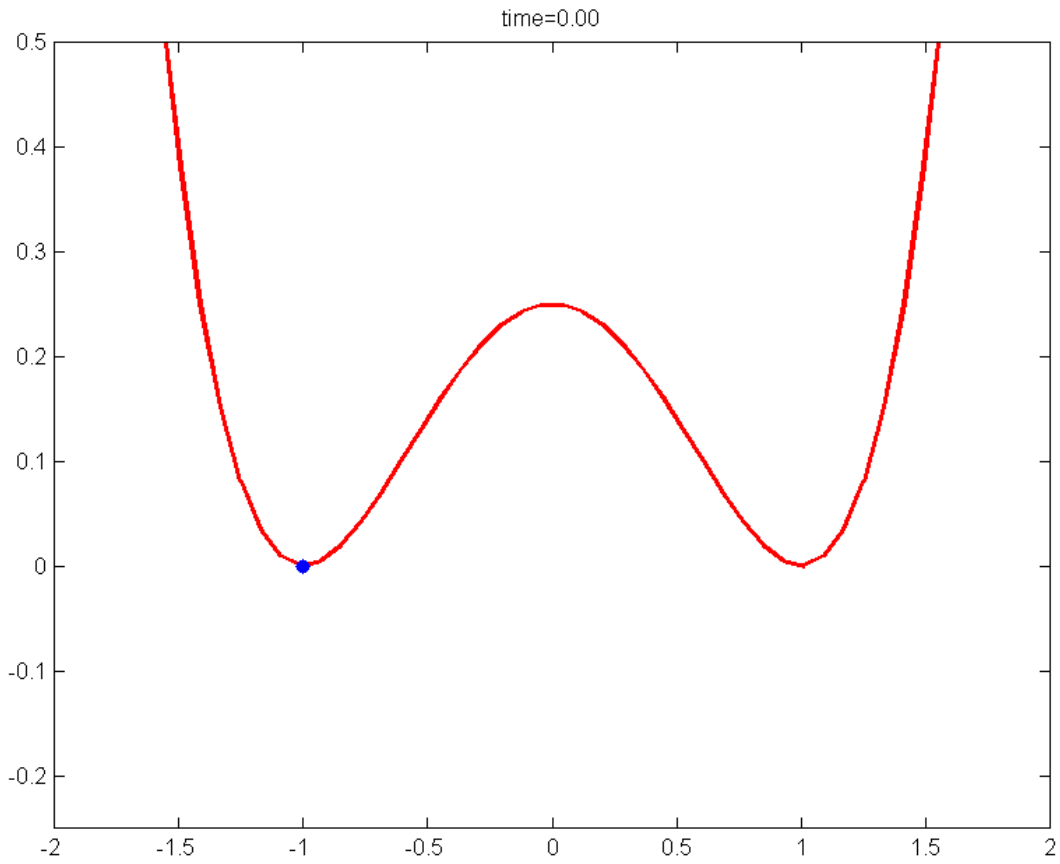

Reaction-rate theory with account of the crystal anharmonicity

Dubinko, Selyshchev, Archilla, Phys. Rev. E. (2011)

$$R_K = \frac{\omega_0}{2\pi}\exp\left[-E_0/k_B T\right]$$ <= Kramers rate

$$U(x,t) = U(x) - (V \cdot x/x_m)\cos(\Omega t)$$

Kramers rate is amplified by:

$I_0\left(V_m/k_B T\right)$ - Bessel function

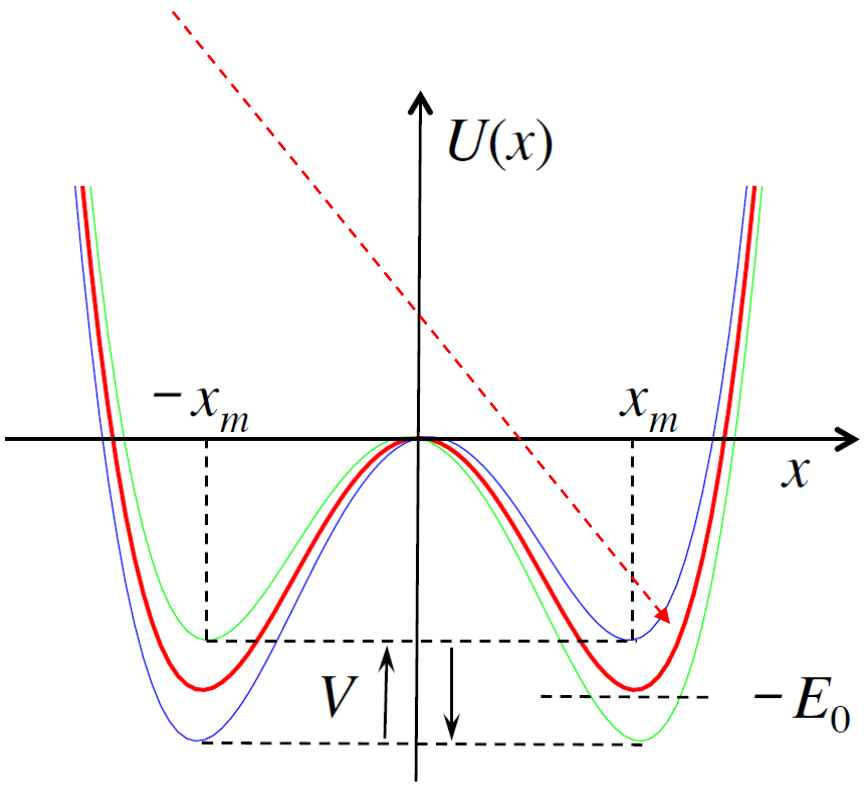

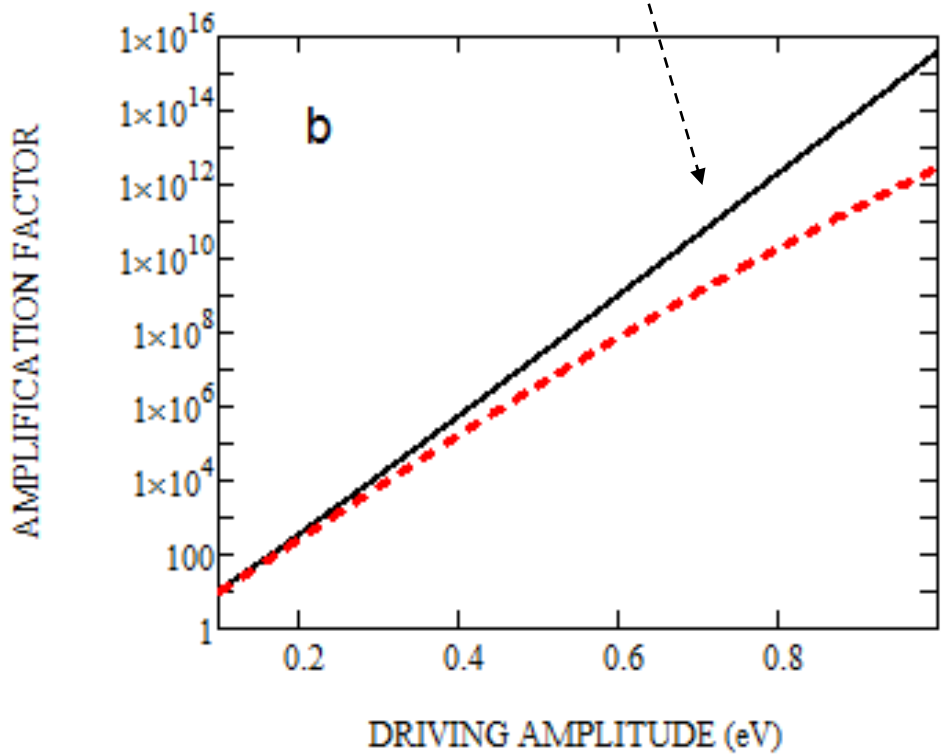

How extend LAV concept to include

Quantum effects, Tunneling

?

Tunneling: Numerical solution of **Schrödinger equation**

Stationary: $t_{Kramers}$~10^5 cycles at $\mathbf{V_{barrier}=12E_0}$

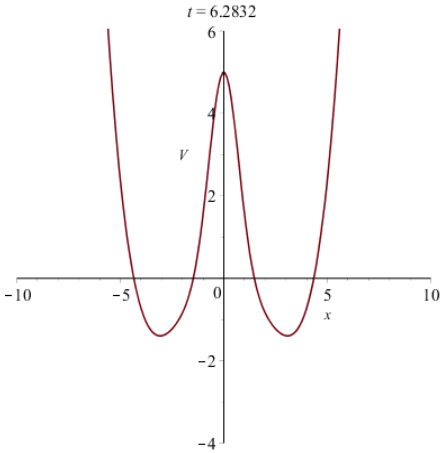

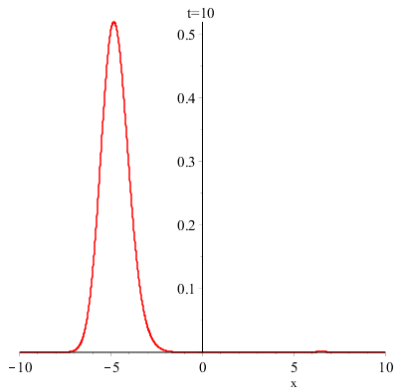

10 cycles

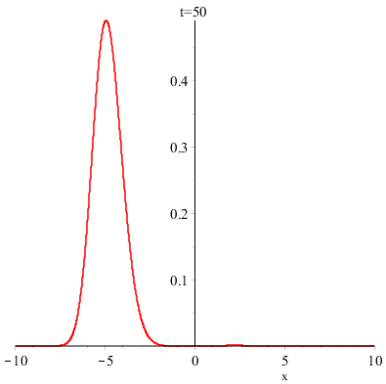

50 cycles

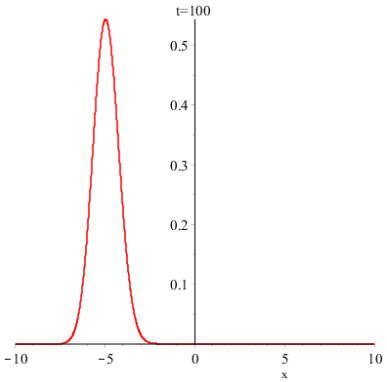

100 cycles

Time-periodically driven: $\mathbf{\Omega = 1.5\ \omega_0\ ,\ g = 0.2}$

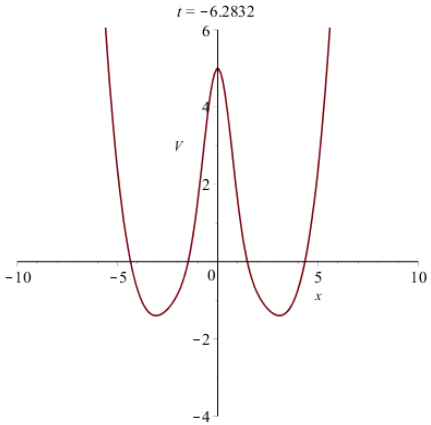

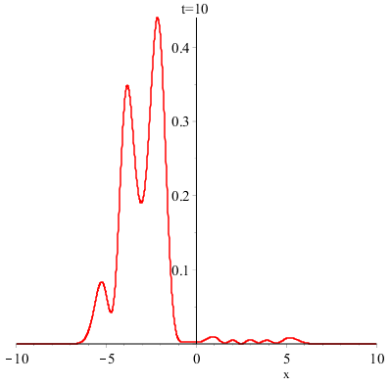

10 cycles

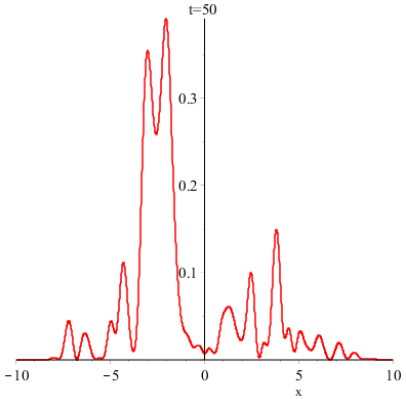

50 cycles

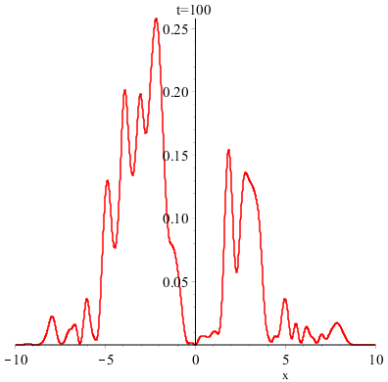

100 cycles

Tunneling as a classical escape rate induced by the vacuum zero-point radiation, A.J. Faria, H.M. Franca, R.C. Sponchiado Foundations of Physics (2006)

The Kramers theory is extended in order to take into account both the action of the thermal and zero-point oscillation (ZPO) energy.

$$R_K = \frac{\omega_0}{2\pi}\exp\left[-E_0/D(T)\right]$$

$$D(T) = E_{ZPO}\coth\left(E_{ZPO}/k_B T\right) \approx \begin{cases} E_{ZPO}, & T \to 0 \\ k_B T, & T >> E_{ZPO}/k_B \end{cases}$$

T – temperature is a measure of *thermal* noise strength

$$E_{ZPO} = \frac{\hbar\omega_0}{2}$$ - ZPO energy is a measure of *quantum* noise strength

When we heat the system we increase temperature, i.e. we increase the *thermal* noise strength

Can we increase
the *quantum* noise strength,
i.e. ZPO energy?

Stationary harmonic potential

$$\langle E \rangle_n = \hbar\omega_0 \left(n + \frac{1}{2} \right)$$

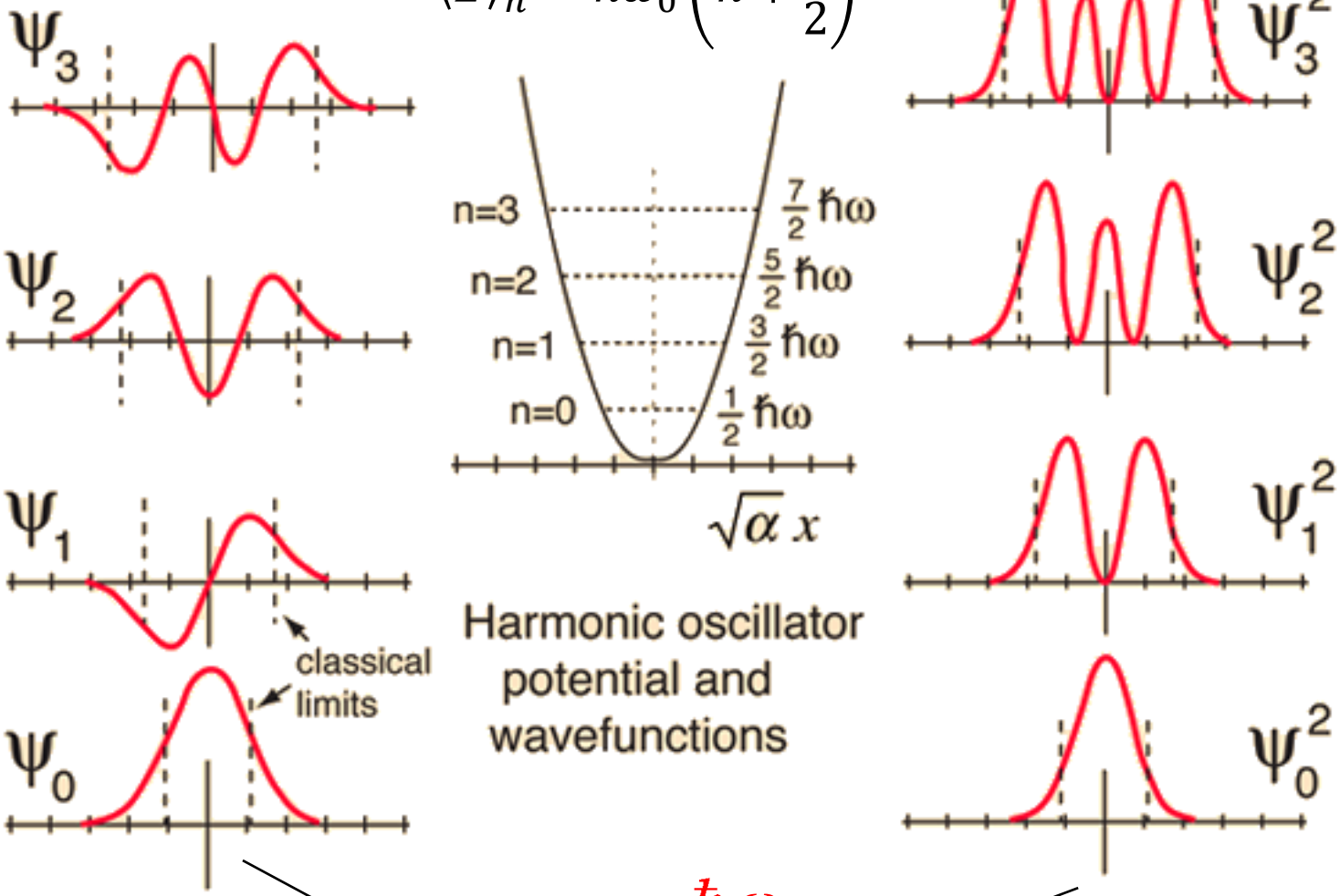

$$E_{ZPO} = \frac{\hbar\omega_0}{2}$$

Time-periodic modulation of the double-well shape changes (i) eigenfrequency and (ii) position of the wells

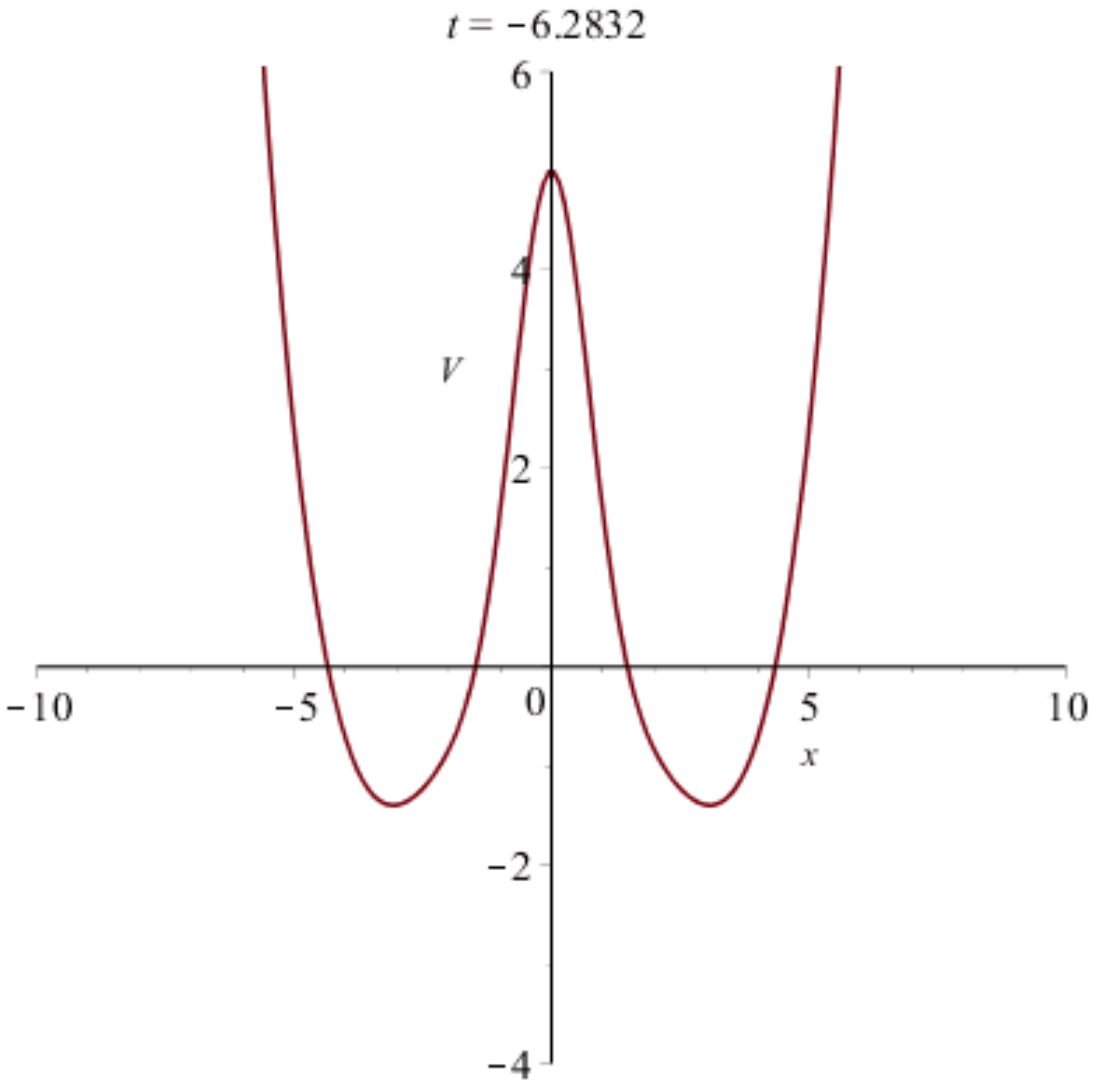

Quasi-energy in time-periodic systems

Consider the Hamiltonian which is periodic in time.

$$i\hbar\frac{\partial\psi}{\partial t}=\hat{H}\psi \qquad \hat{H}(t+T)=\hat{H}(t)$$

It can be shown that Schrodinger equation has class of solutions in the form:

$$\psi_\alpha(t+T)=\exp(-i\alpha)\psi_\alpha(t)$$

where $\varepsilon=\frac{\hbar\alpha}{T}$ Is the quasi-energy

$$i\hbar\frac{\partial}{\partial t}\psi(x,t)=-\frac{\hbar^2}{2m}\frac{\partial^2}{\partial x^2}\psi(x,t)+\frac{m\omega^2(t)}{2}x^2\psi(x,t)$$

$$\varepsilon_n=\left(n+\frac{1}{2}\right)\lambda(\omega(t))$$

Time-periodic driving of the harmonic oscillator with non resonant frequencies **$\Omega \neq 2\omega_0$** renormalizes its energy spectrum, which remains equidistant, but the quasi-energy quantum $\lambda(\omega(t))$ becomes a function of the driving frequency

Time-periodic modulation of the double-well shape changes (i) eigenfrequency and (ii) position of the wells

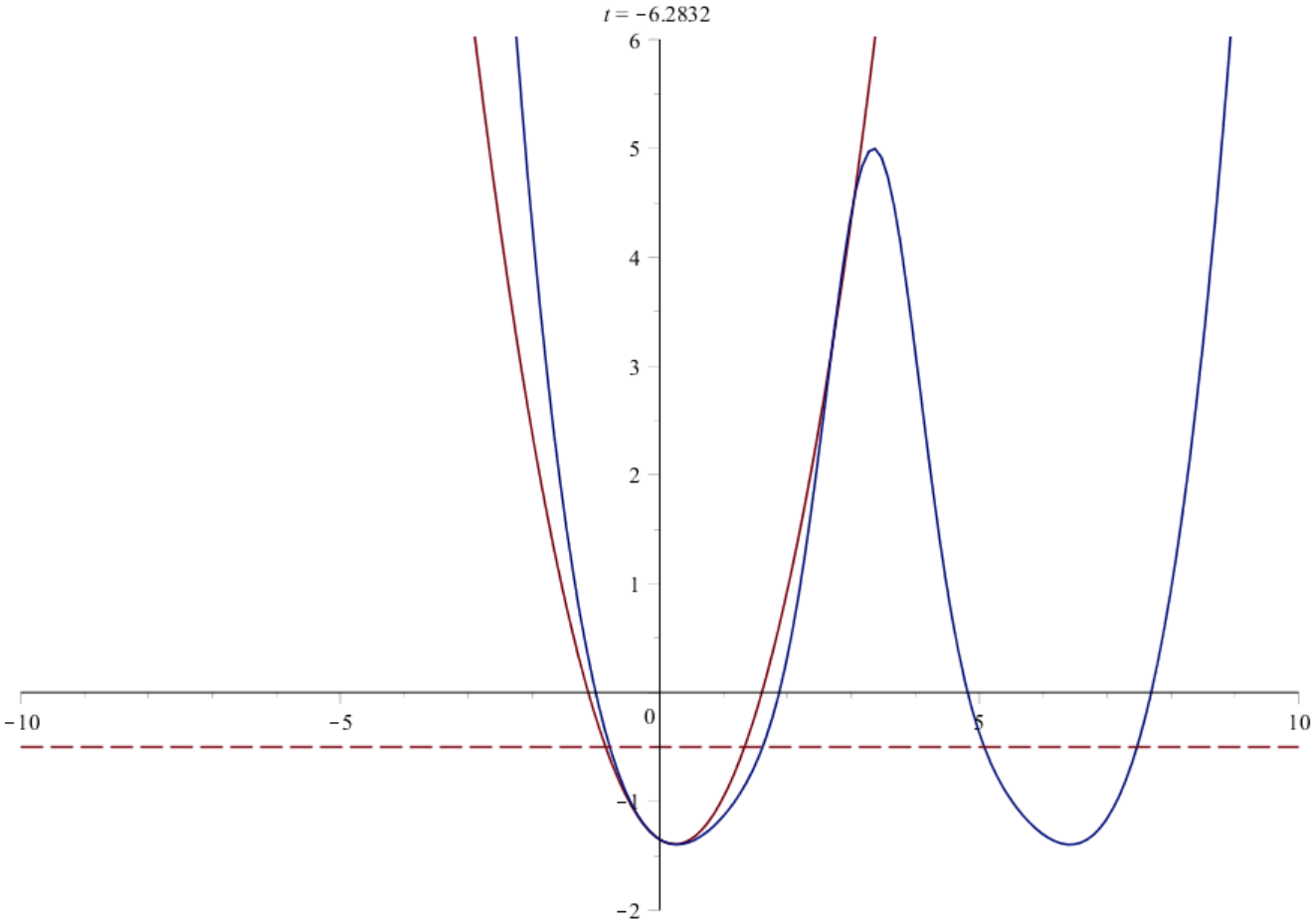

Parametric resonance with **time-periodic eigenfrequency $\Omega = 2\omega_0$**

$$i\hbar\frac{\partial\psi}{\partial t} = -\frac{\hbar^2}{2m}\frac{\partial^2\psi}{\partial x^2} + \frac{m\omega^2(t)}{2}x^2\psi$$

Schrödinger equation

$$\psi(x_0, t_0 = 0) = \frac{1}{\sqrt[4]{2\pi\sigma_0}}\exp\left(-\frac{x_0^2}{4\sigma_0}\right)$$

Initial Gaussian packet $\sigma_0 = \dfrac{\hbar}{2m\omega_0}$

Parametric regime $\Omega = 2\omega_0$:

$$\ddot{x} + \omega_0^2\left[1 - g\cos(2\omega_0 t)\right]x = 0$$

g << 1 – modulation amplitude

$$\sigma_x(t) = \sigma_0\cosh\left(\frac{g\omega_0 t}{2}\right)\left[1 + \tanh\left(\frac{g\omega_0 t}{2}\right)\sin(2\omega_0 t)\right]$$

dispersion

ZPO energy:

$$E_{ZPO}(t) = \frac{\hbar\omega_0}{2}\cosh\frac{g\omega_0 t}{2}$$

ZPO amplitude:

$$\Lambda_{ZPO}(t) = \sqrt{\frac{\hbar}{2m\omega_0}\cosh\frac{g\omega_0 t}{2}}$$

Non-stationary harmonic potential with **time-periodic eigenfrequency $\Omega = 2\omega_0$**

$$\Lambda_{ZPO}(t) = \sqrt{\frac{\hbar}{2m\omega_0}\cosh\frac{g\omega_0 t}{2}}$$

$$E_{ZPO}(t) = \frac{\hbar\omega_0}{2}\cosh\frac{g\omega_0 t}{2}$$

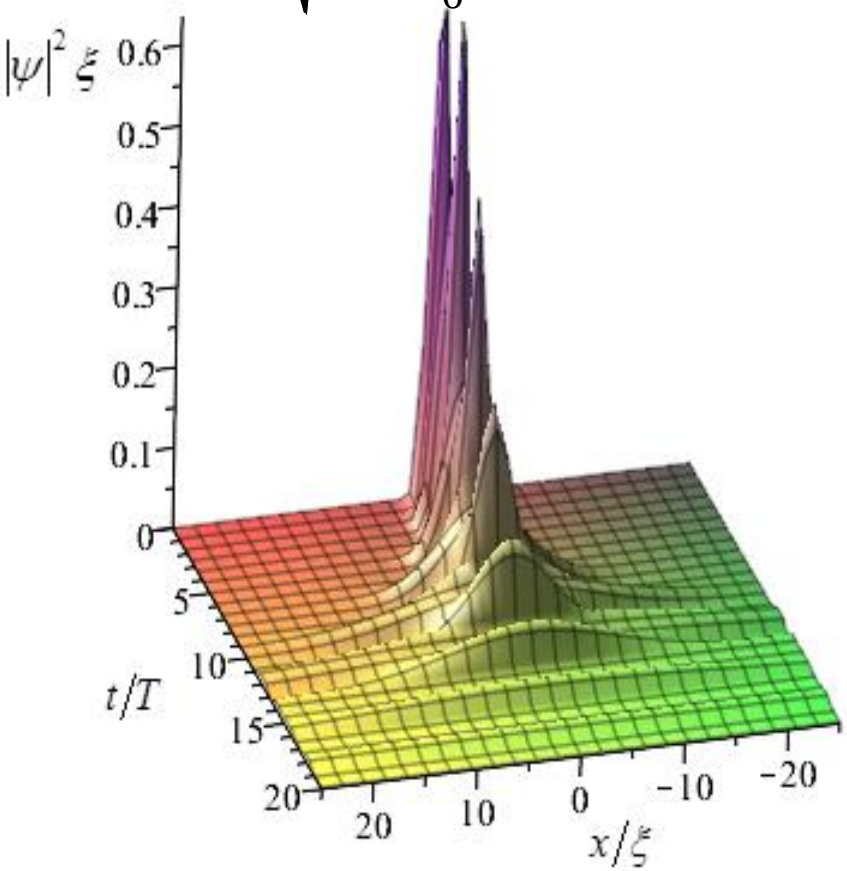

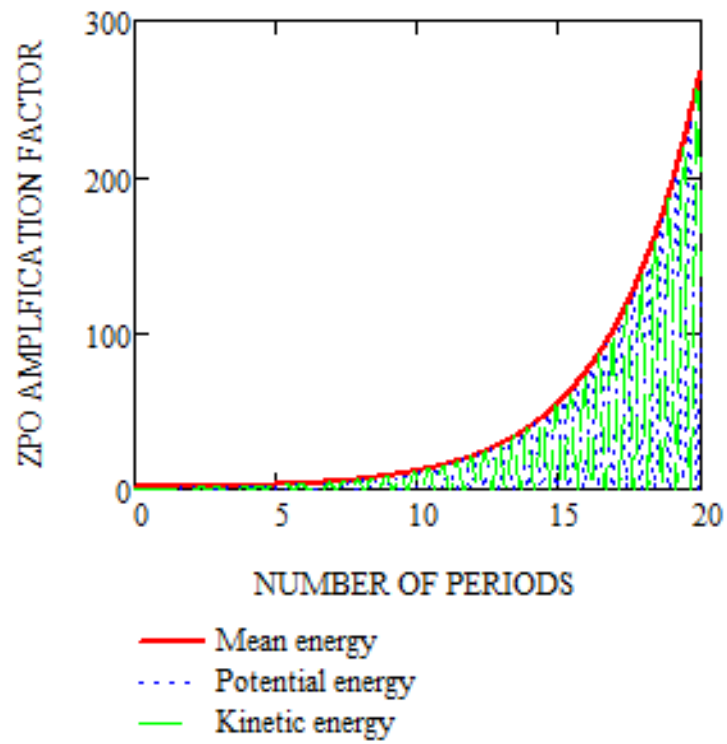

$$\langle E\rangle_{theor}(t) \approx \hbar\omega_0\left(n+\frac{1}{2}\right)\cosh\frac{g\omega_0 t}{2}$$

$$g \ll 1$$

General case: n = 0,1,2, …

$$\langle E\rangle_{num}(t) = \frac{\hbar\omega_0}{2}\left(n+\frac{1}{2}\right)\left[\frac{\dot{Y}^2+\omega_0^2\dot{Z}^2}{\omega_0^2}+\frac{\omega^2(t)}{\omega_0^2}\left(Y^2+\omega_0^2 Z^2\right)\right]$$

$$g = 0.1, \qquad n = 0$$

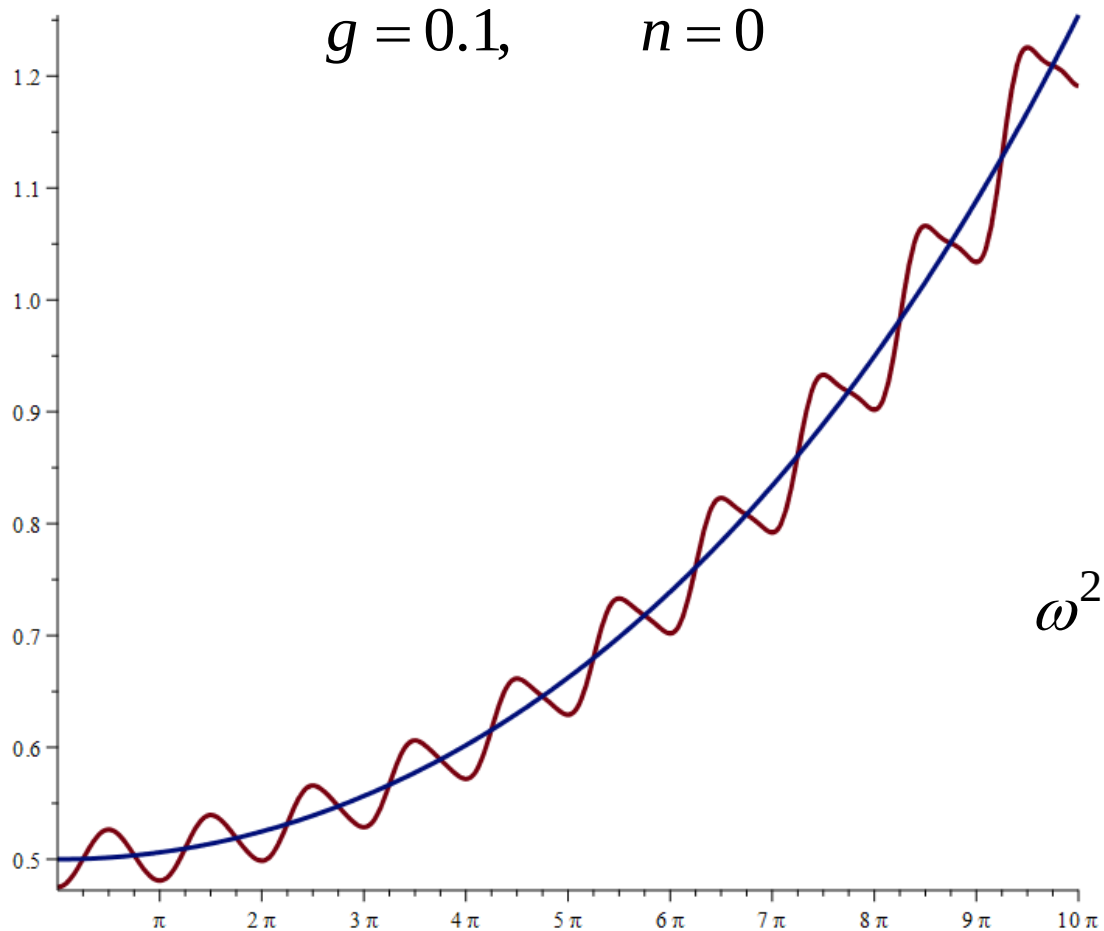

$$\begin{cases}\ddot{Y}(t)+\omega^2(t)Y(t)=0\\ \dot{Y}(0)=0, \qquad Y(0)=1\end{cases}$$

$$\begin{cases}\ddot{Z}(t)+\omega^2(t)Z(t)=0\\ \dot{Z}(0)=1, \qquad Z(0)=0\end{cases}$$

$$\omega^2(t)=\omega_0^2\left[1-g\cos(2\omega_0 t)\right]$$

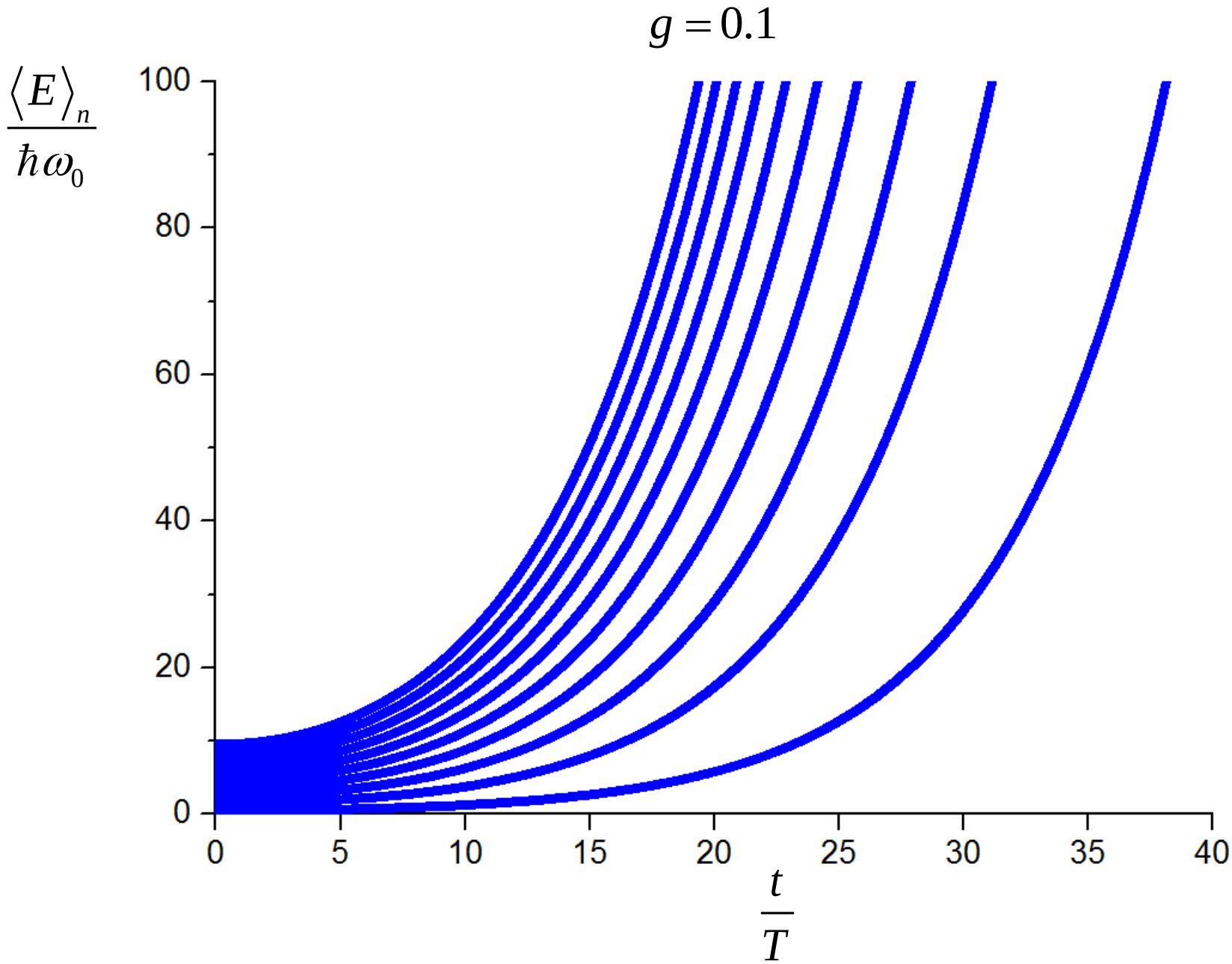
$g = 0.1$
$\frac{\langle E \rangle_n}{\hbar\omega_0}$
100
80
60
40
20
0
0
5
10
15
20
25
30
35
40
$\frac{t}{T}$

Non-stationary harmonic potential with **time-periodic** shifting of the **well position at $\Omega = \omega_0$**

$$\langle E \rangle = \frac{\hbar\omega_0}{2} + \frac{\left(g_A A_{ZPO}\right)^2 m\omega_0^2}{8}\left[\omega_0^2 t^2 + \omega_0 t \sin 2\omega_0 t + \sin^2 \omega_0 t\right]$$

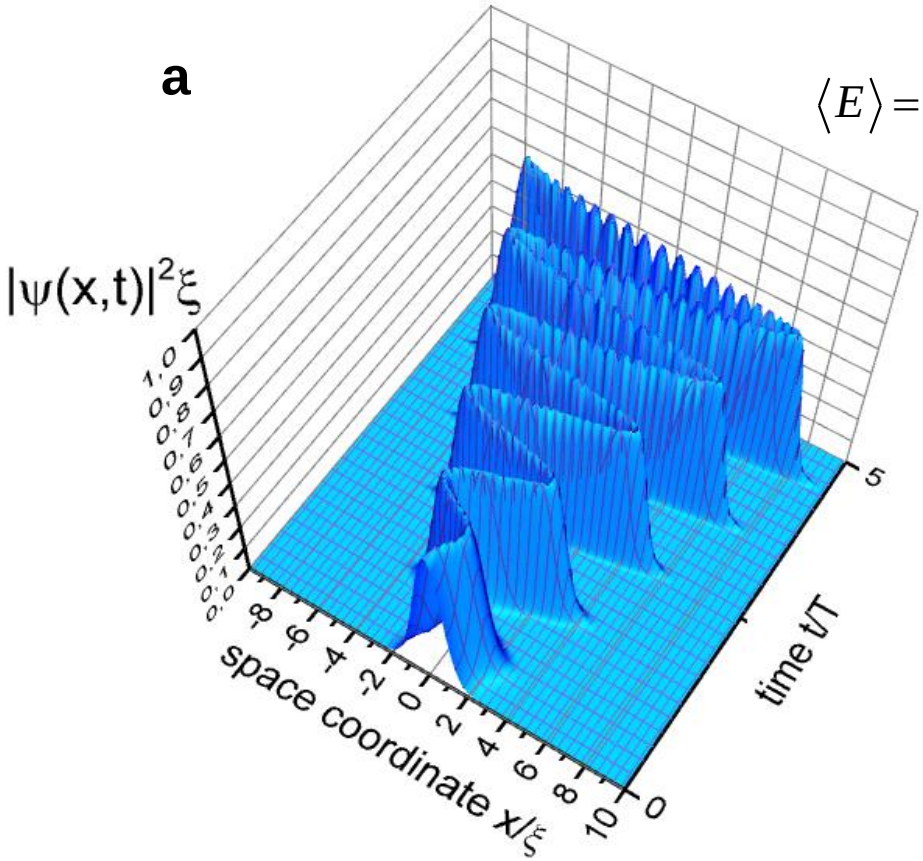

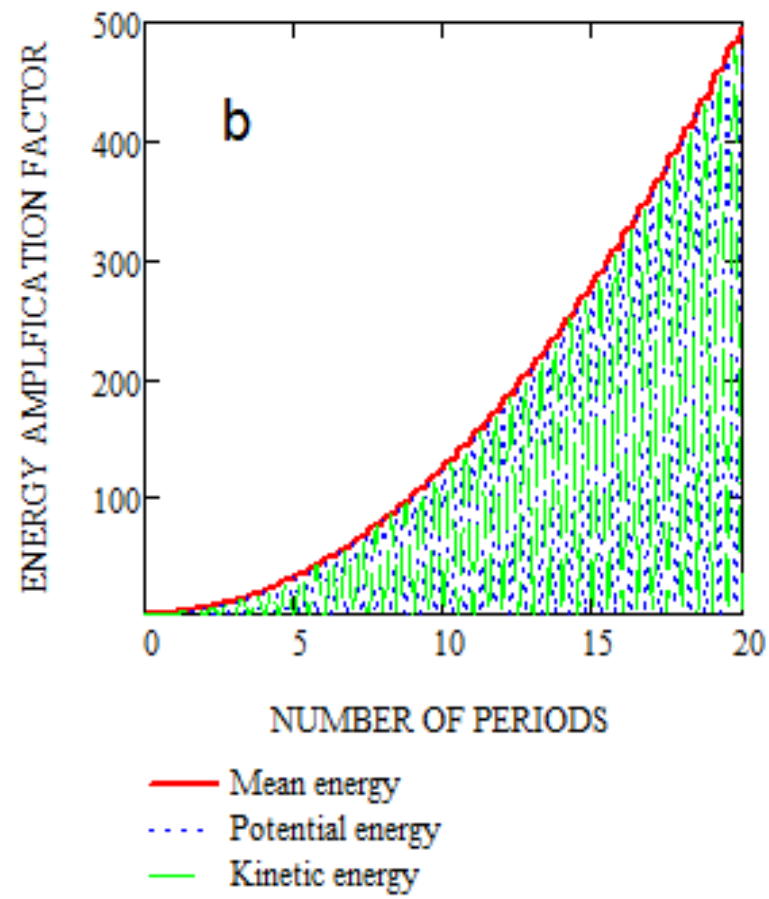

$$\lambda(t) = \frac{g_A A_{ZPO}}{2}\omega_0 t\left(\cos\omega_0 t - \frac{\sin\omega_0 t}{\omega_0 t}\right)$$

Extreme example – Low Energy Nuclear Reactions (LENR)

Electrolysis

"Water will be the coal of the future"

Jules Verne

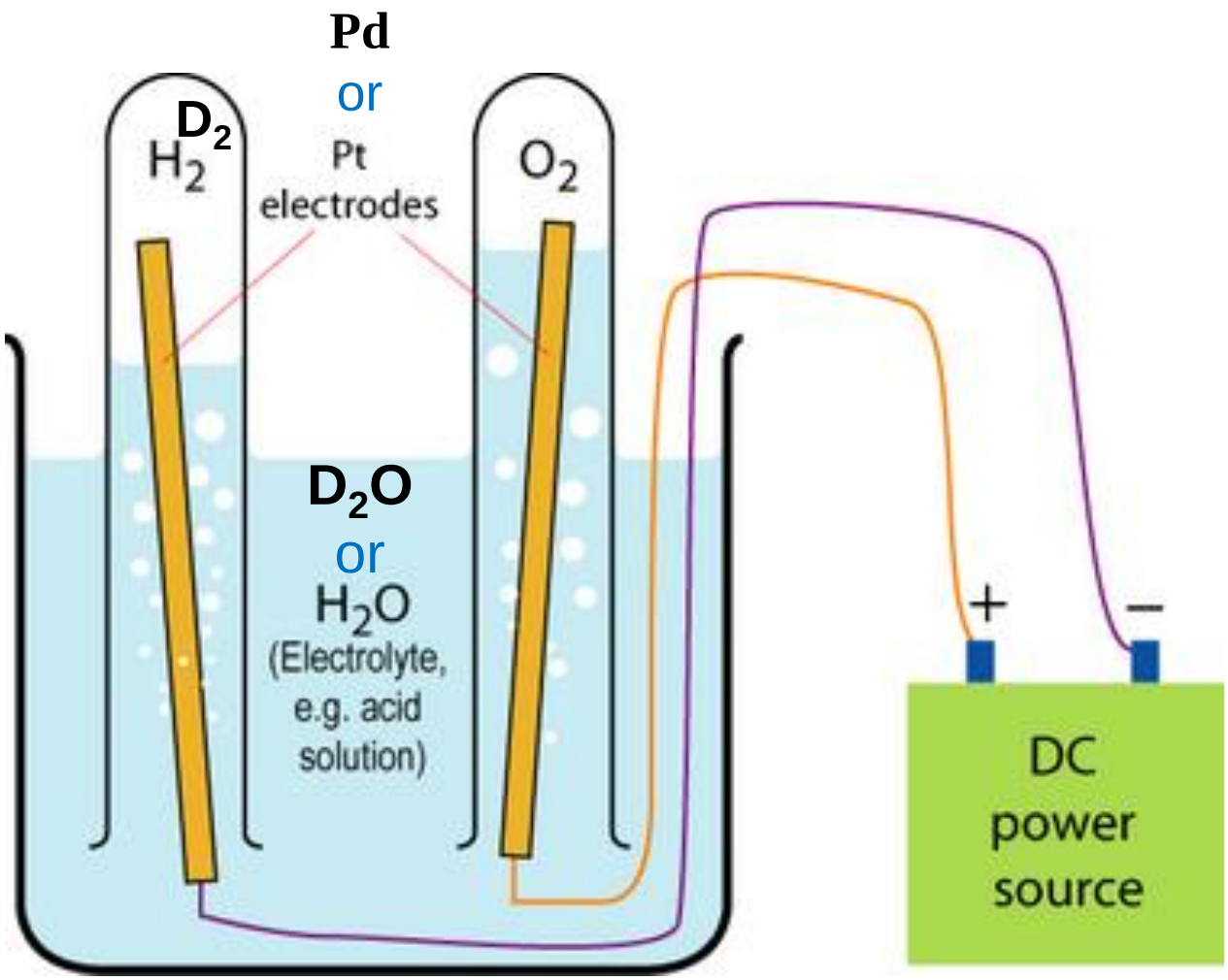

LENR requirements for D_2O electrolysis

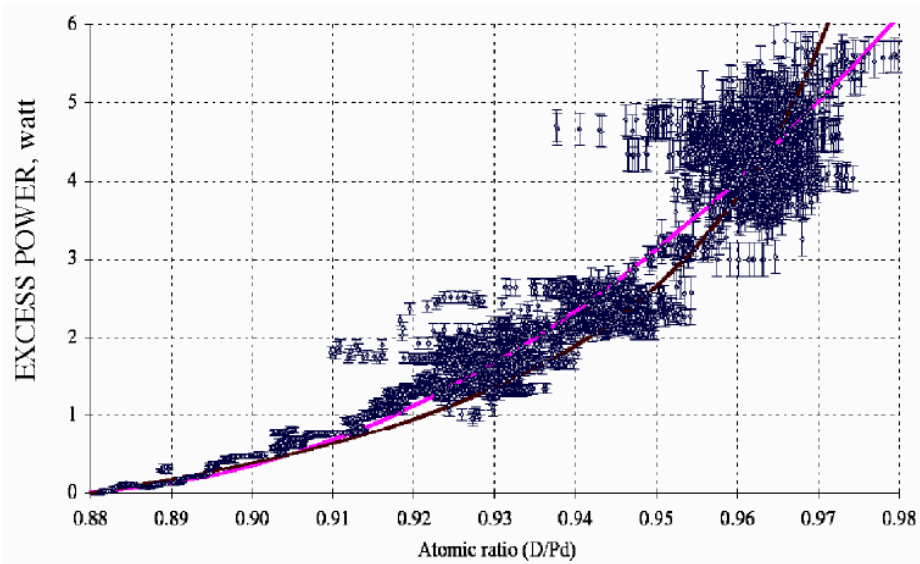

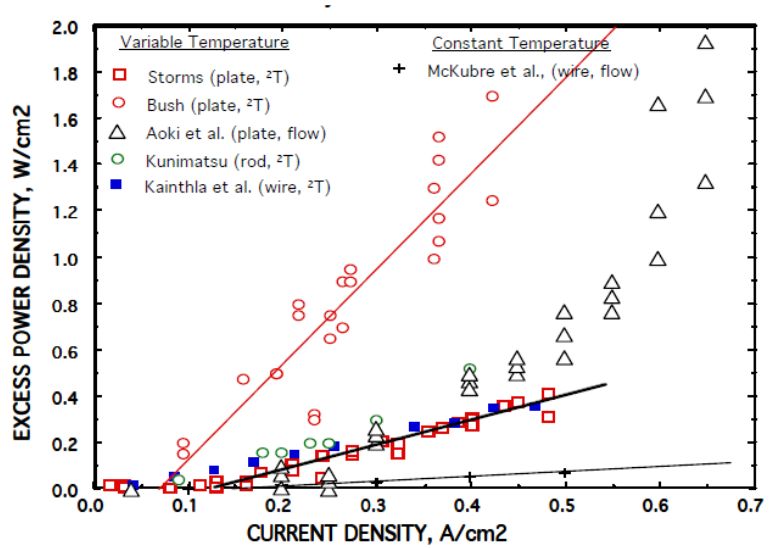

(i) high loading of D > 0.88

(ii) external driving

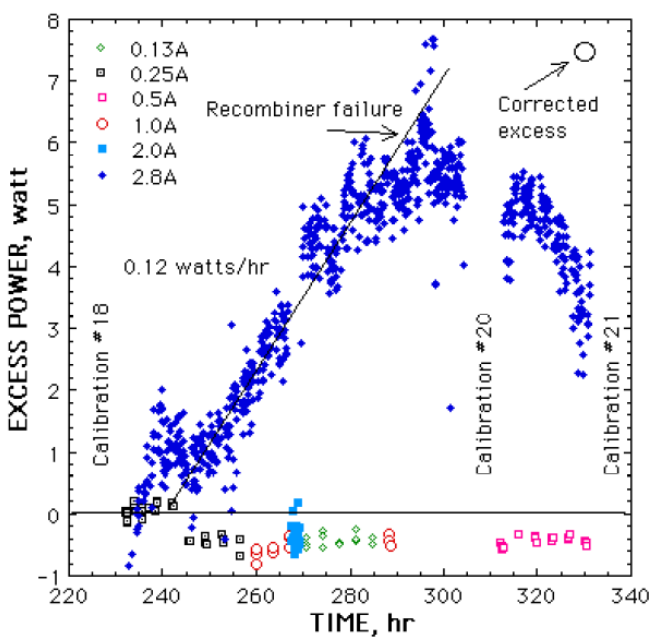

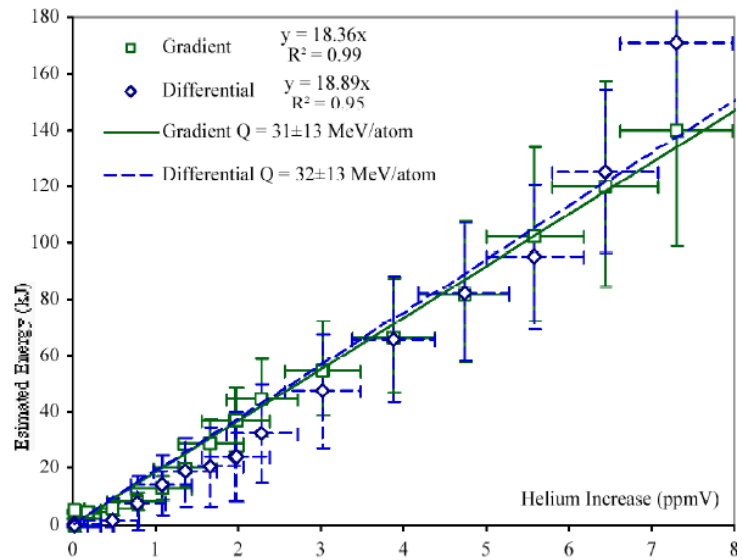

$D + D \rightarrow {}^{4}He + 23.8\ MeV_{lattice}$

Anomalous Excess Heat Generation by the Interaction between Nano-structured Pd/Ni surface and D_2/H_2 gas

Yasuhiro Iwamura[1], Takehiko Itoh[1,2], Jirohta Kasagi[1] and Hiroki Shishido[3]

1 Research Center for Electron Photon Science, Tohoku University, 982-0826 Japan

2 CLEAN PLANET Inc., 105-0022 Japan

3 Department of Quantum Science and Energy Engineering,
Graduate School of Engineering, Tohoku University, Sendai 980-8579, Japan

12th International Workshop on Anomalies in Hydrogen Loaded Metals
Hotel Langhe e Monferrato, Via Contessa di Castiglione,14055 Costigliole d'Asti (AT), Italy. 5-9 June 2017

Dr. Mizuno's Experiment

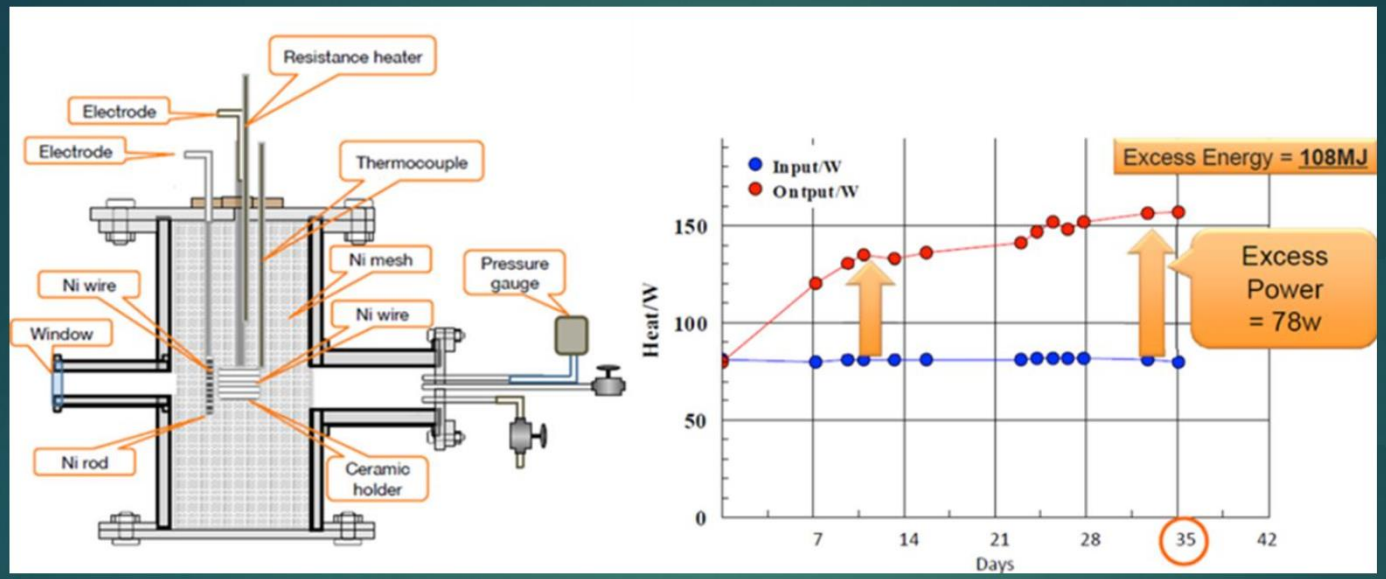

1. Make Pd/Ni Nano Structure Surface in the chamber using Plasma Discharge
2. D_2/H_2 gas Introduced Chamber
3. Observe Anomalous Excess Heat Generated

[1] T. Mizuno, "REACTANT, HEATING DEVICE, AND HEATING METHOD", Patent Application, WO2015/008859 A2.
[2] H. Yoshino, E. Igari and T.Mizuno, Presentation at 2014 CF/LANR Colloquium at MIT, March.21-23, 2014, Massachusetts Institute of Technology, Cambridge, MA, USA.

Fabricated Nano–structured Ni and Pd Surface

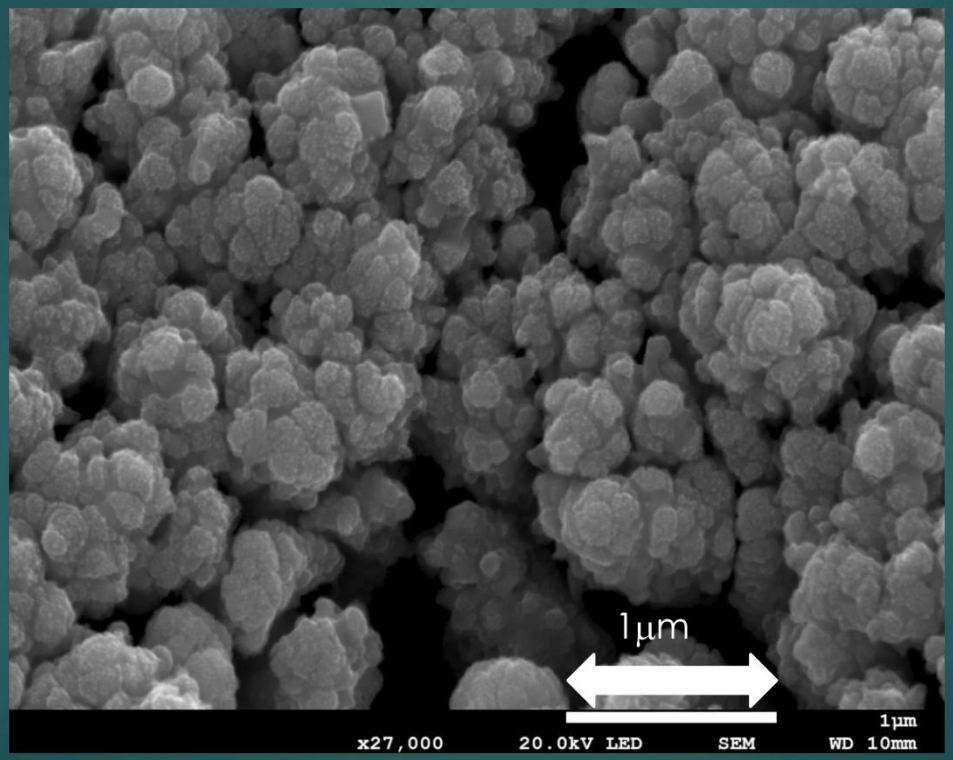

Why LENR is unbelievable?

G. Gamow, "Zur Quantentheorie des Atomkernes", *Z. Phys.*, **51**, 204–212 (1928).

$$G \approx \exp\left\{-\frac{2}{\hbar}\int_{r_0}^{R_c} dr\sqrt{2\mu\left(V(r)-E\right)}\right\}$$

Gamow factor

$$r_0 \sim 3\ \text{fm}$$

Nuclear radius deduced from **scattering experiments**

$$V(R_0) = \frac{e^2}{r_0} \approx 450\ \text{keV}$$

Coulomb barrier

At any crystal Temperature:

$$E << V(r_0) \Rightarrow G \approx 10^{-2760}$$

HOWEVER, is the Coulomb barrier that huge in the lattice **?**

Willis Eugene *Lamb*
Nobel Prize 1955

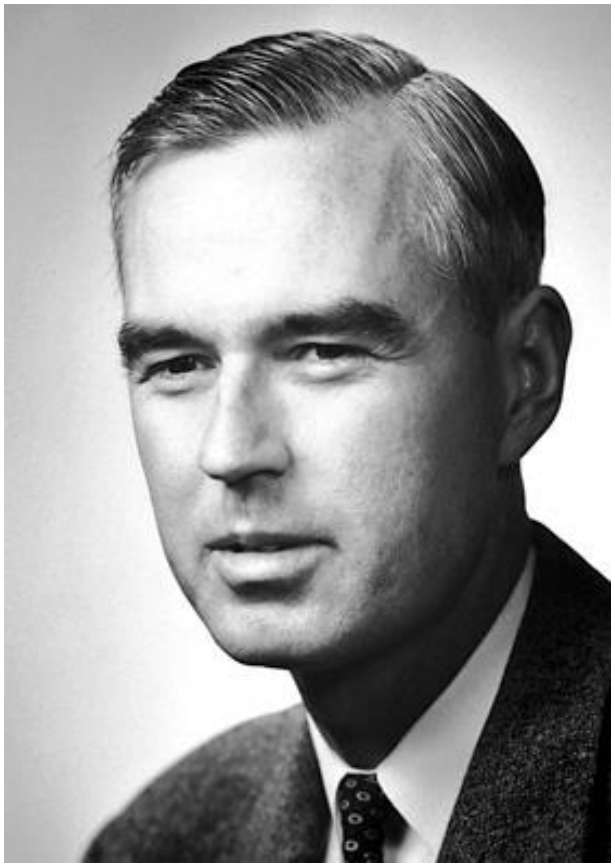

R.H. Parmenter, **W.E. Lamb**,
Cold fusion in Metals (1989)
Electron screening

Julian Schwinger
Nobel Prize 1965

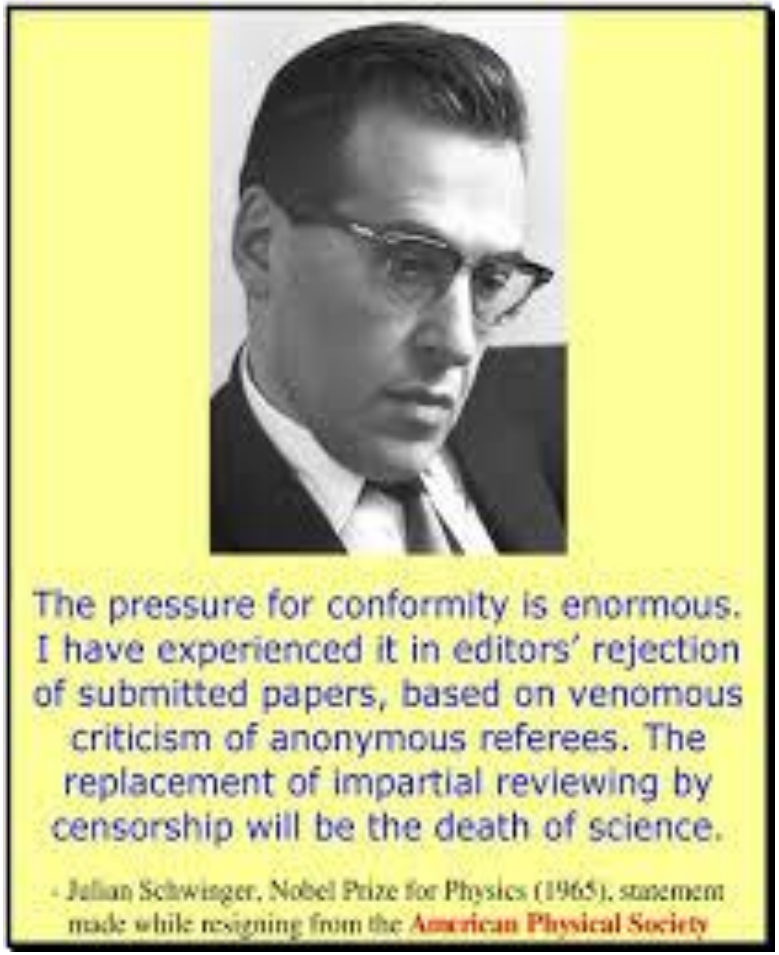

J. Schwinger, Nuclear Energy in an Atomic Lattice (1990)
Lattice screening

J. Schwinger, *Nuclear Energy in an Atomic Lattice* I, Z. Phys. D 15, 221 (**1990**)

Effective Coulomb repulsion with account of **zero-point oscillations**

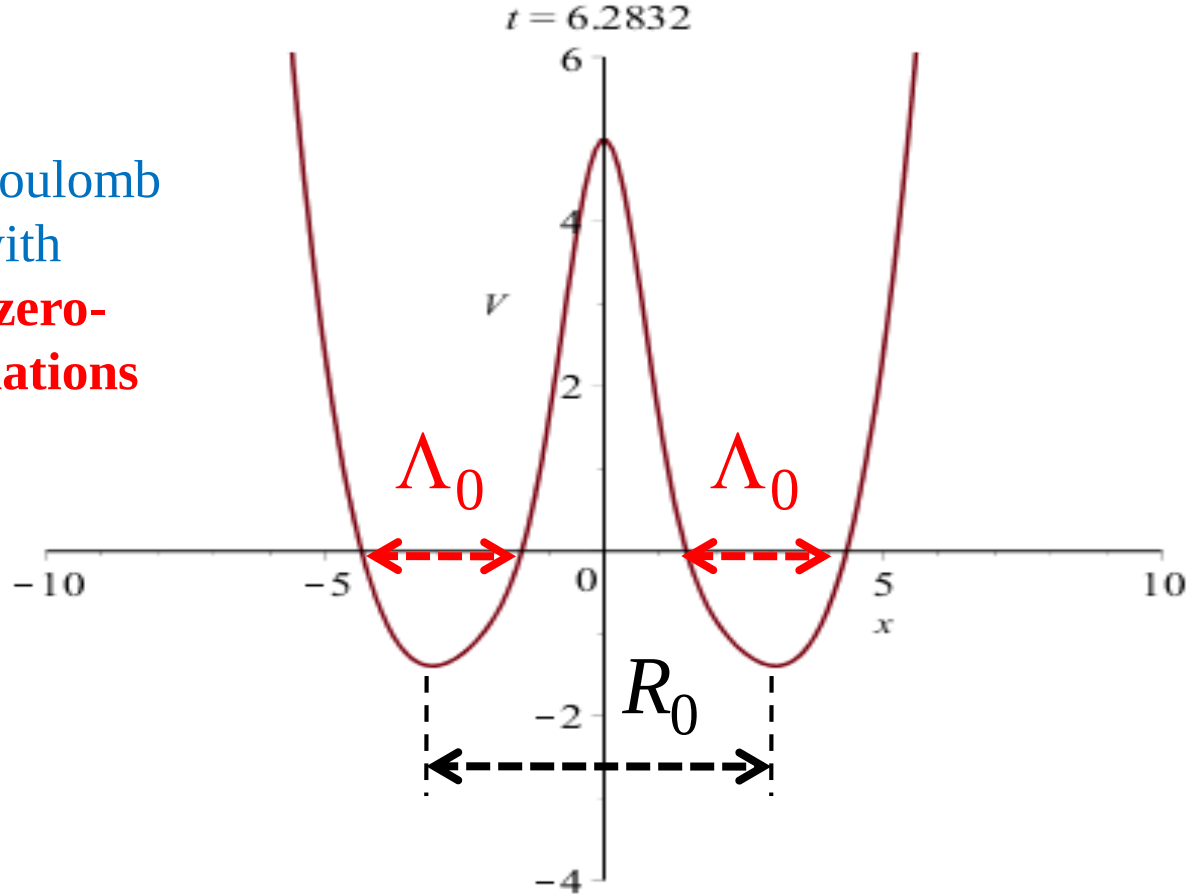

$$ {}_0\langle V_c(r)\rangle_0 = \frac{e^2}{r}\sqrt{\frac{2}{\pi}}\int_0^{r/\Lambda_0} dx \exp\left(-\tfrac{1}{2}x^2\right) \approx \begin{cases} r \gg \Lambda_0 : \dfrac{e^2}{r} \\ r \ll \Lambda_0 : \left(\dfrac{2}{\pi}\right)^{1/2} \dfrac{e^2}{\Lambda_0} \end{cases} $$

~ **100 eV** (!!!)

J. Schwinger, *Nuclear Energy in an Atomic Lattice* The First Annual Conference on Cold Fusion. University of Utah Research Park, Salt Lake City (**1990**)

D-D fusion rate in Pd-D lattice: $\upsilon_{D-D} = \frac{1}{T_0} = \left(2\pi/\hbar\right)_0 \left\langle V\delta\left(H-E\right)V\right\rangle_0$

T_0 is the mean lifetime of the *phonon vacuum* state before releasing the nuclear energy **directly** to the lattice **(no radiation!)**:

$$\frac{1}{T_0} \approx 2\pi\omega_0 \left(\frac{2\pi\hbar\omega_0}{E_{nucl}}\right)^{\frac{1}{2}} \left(\frac{r_{nucl}}{\Lambda_0}\right)^3 \exp\left[-\frac{1}{2}\left(\frac{R_0}{\Lambda_0}\right)^2\right] \sim 10^{-19}\, s^{-1} \div 10^{-30}\, s^{-1}$$

$$\Lambda_0 = 0.1\text{A} \qquad R_0 = 0.94\text{A} \div 2.9\text{A}$$

Schwinger, ***Nuclear Energy in an Atomic Lattice*** I, Z. Phys. D 15, 221 (**1990**).

Parmenter, **Lamb**, Cold fusion in Metals, Proc. Natl. Acad. Sci. USA, v. 86**,** 8614-8617 (**1989**).

$$V_{eff}(r) \approx \frac{m\omega_0^2}{2} r^2 + \frac{e^2}{R_0 - r} \exp\left(-\frac{R_0 - r}{\lambda_D}\right) \sqrt{\frac{2}{\pi}} \int_0^{(R_0 - r)/\Lambda_0} dx \exp\left(-\tfrac{1}{2} x^2\right)$$

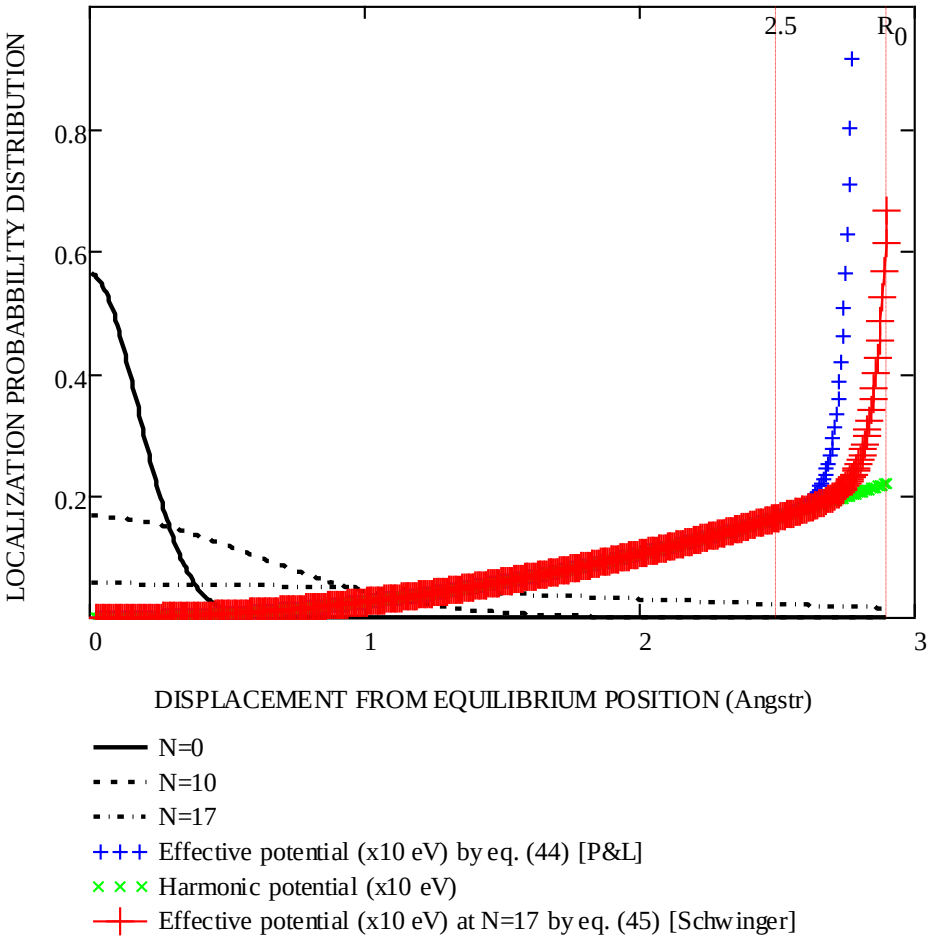

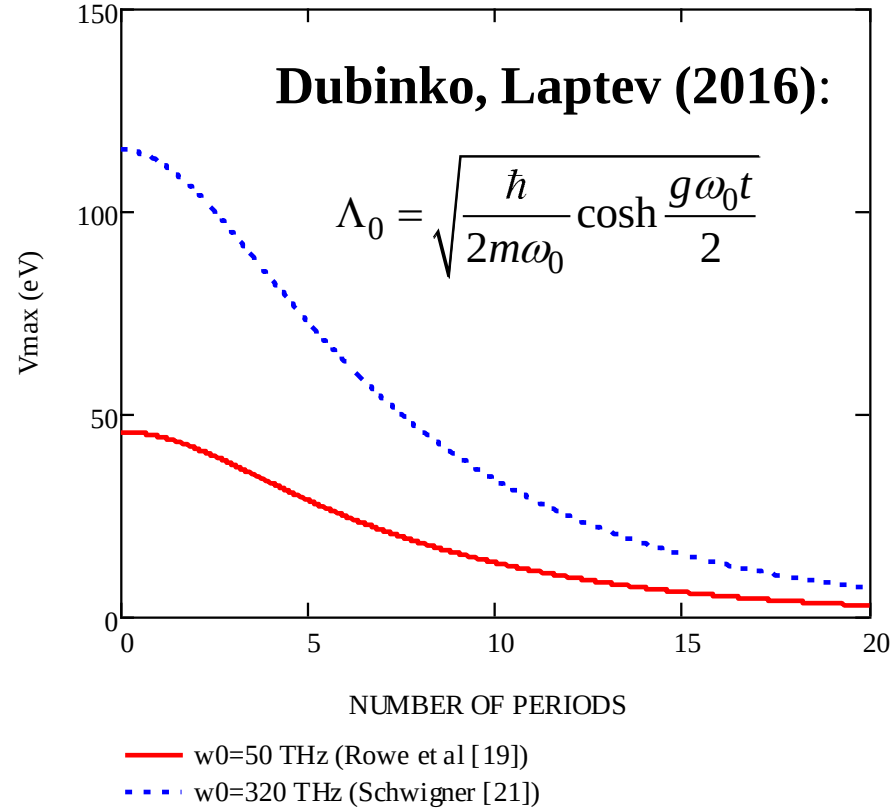

Schwinger, *Nuclear energy in an atomic lattice*. Proc. Cold Fusion Conf. (1990)
Dubinko, Laptev, *Chemical and nuclear catalysis driven by LAVs*, LetMat (2016)

$$\frac{1}{T} \approx 2\pi\omega_0 \left(\frac{2\pi\hbar\omega_0}{E_{nucl}}\right)^{\frac{1}{2}} \left(\frac{r_{nucl}}{\Lambda}\right)^3 \exp\left[-\frac{1}{2}\left(\frac{R_0}{\Lambda_0}\right)^2\right]$$

$$\Lambda_0 = \begin{cases} \sqrt{\dfrac{\hbar}{2m\omega_0}} = const \\ \sqrt{\dfrac{\hbar}{2m\omega_0}\cosh\dfrac{g\omega_0 t}{2}} \end{cases}$$

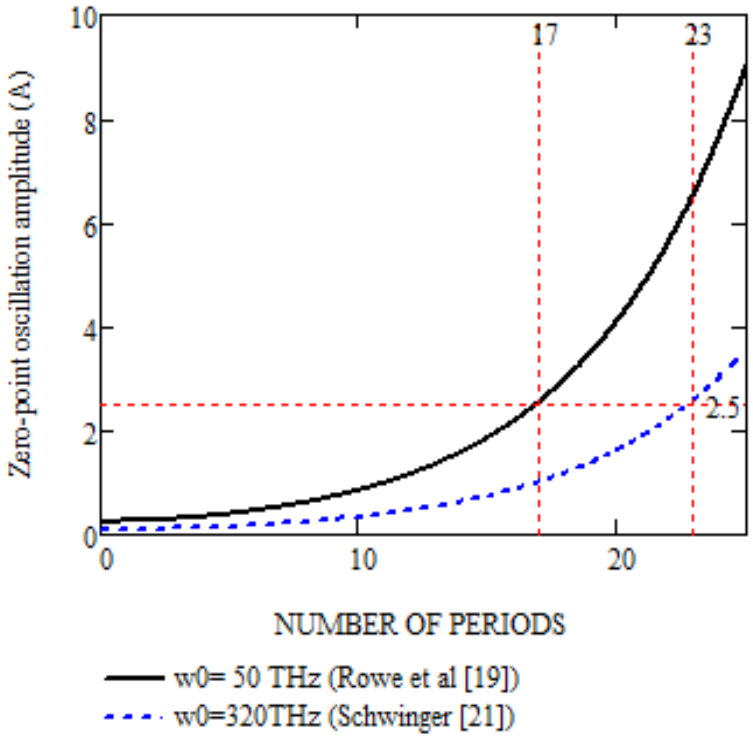

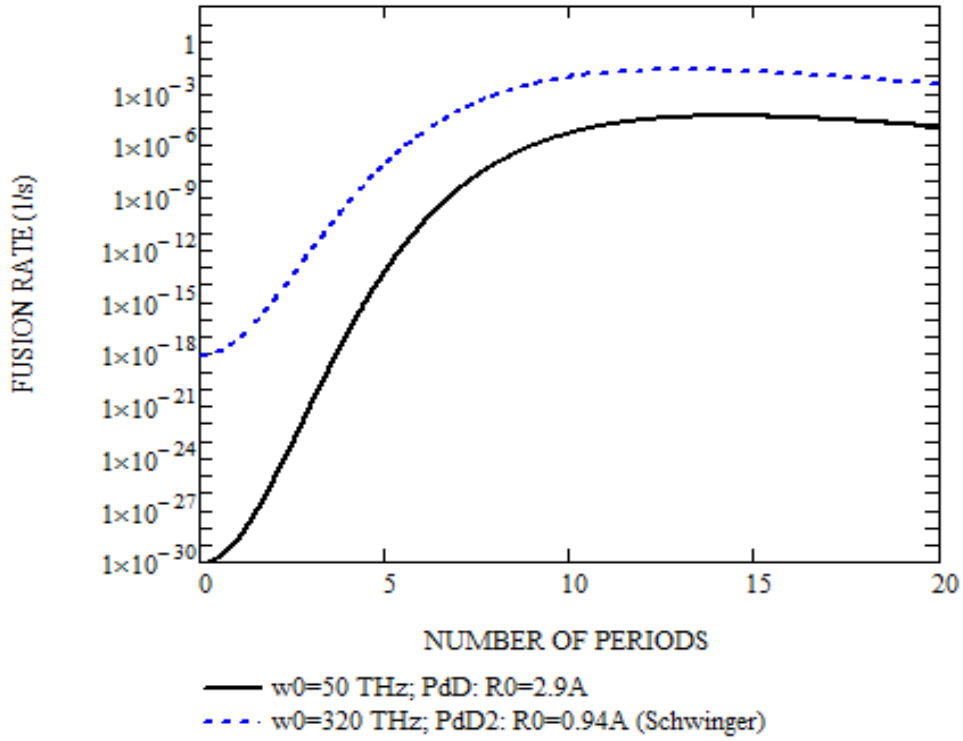

LENR power density under D_2O electrolysis

$$P_{D-D}(T,J) = K_{DB}^{J}\left(E_{DB}^{*},T,J\right)E_{D-D}$$

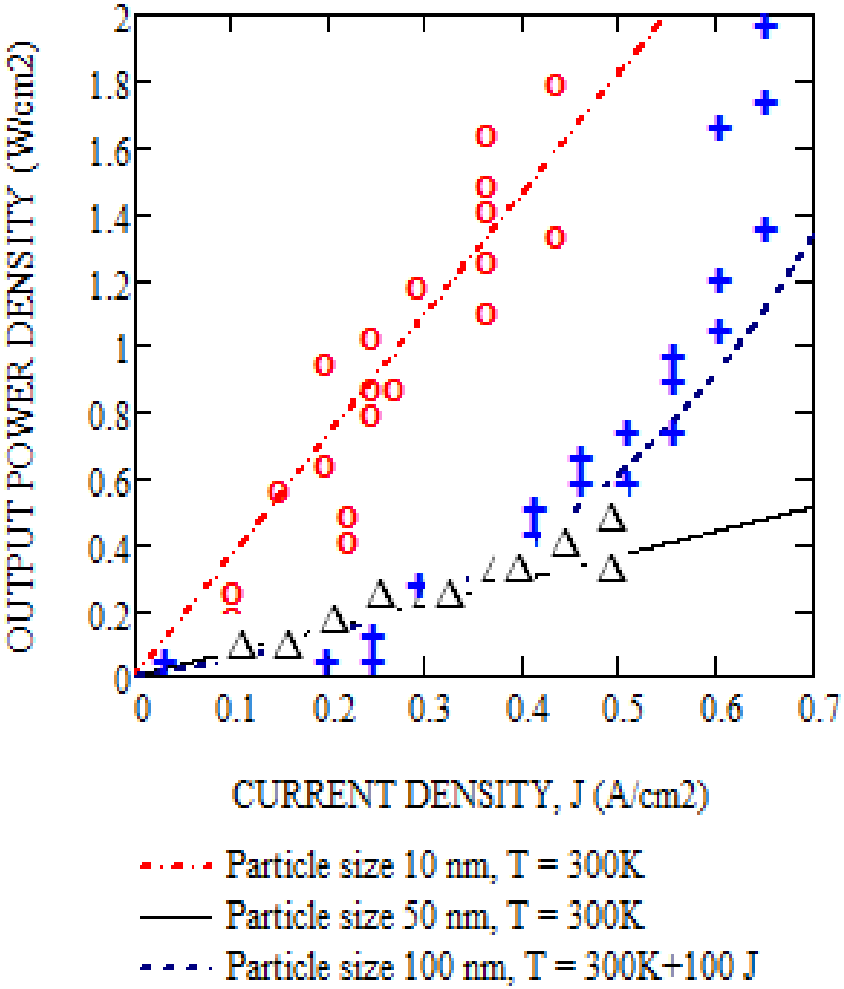

Table 1

Parameter	Value
D-D equilibrium spacing in PdD, b (Å)	2.9
DB excitation efficiency, k_{eff}	10^{-10}
Fusion energy, (MeV)	23.8
Mean DB energy, (eV)	1
DB oscillation frequency, ω_{DB} (THz)	20
Critical DB lifetime, τ_{DB} (ps/cycles)	10/100
Quodon excitation energy (eV)	0.8
Quodon excitation time, τ_{ex} (ps/cycles)	1/10
Quodon propagation range, l_q (nm)	2.9
Cathod size/thickness (mm)	5

BNC can provide up to 10^{14} "collisions" per cm^3 per second

MD modeling of LAVs in NiH and PdH crystals and Pd nanocrystals

Visualization of the Pd(Ni)H fcc Lattice (NaCl type)

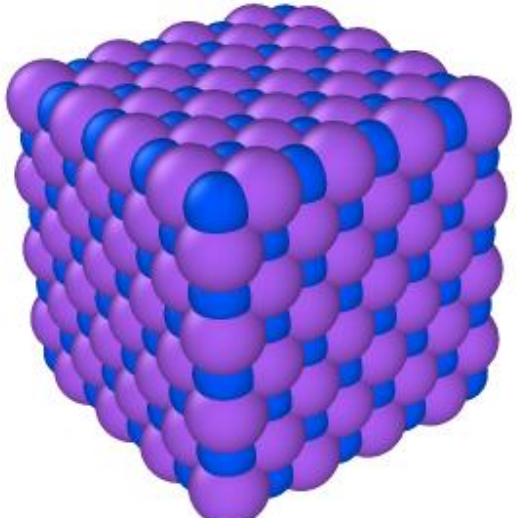

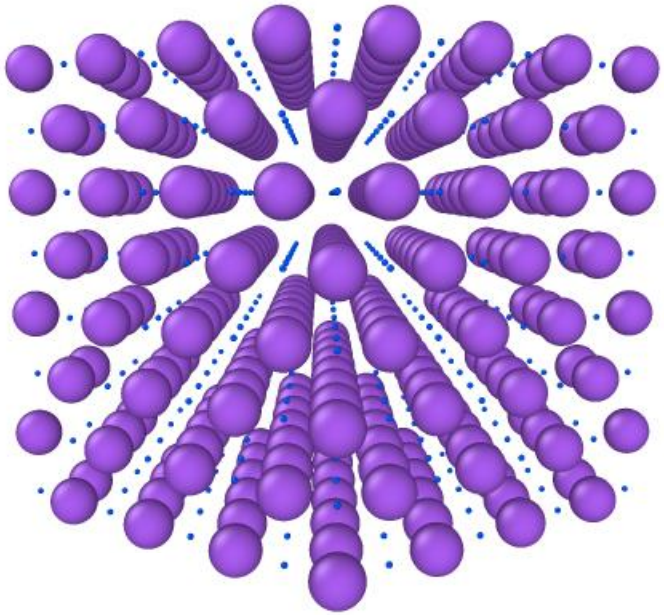

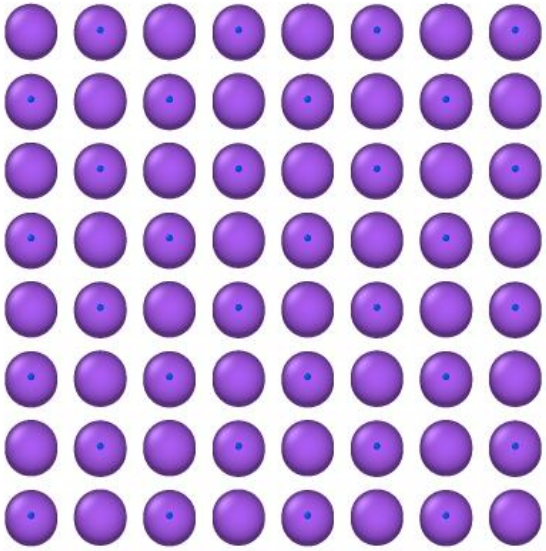

Density Of States of NiH

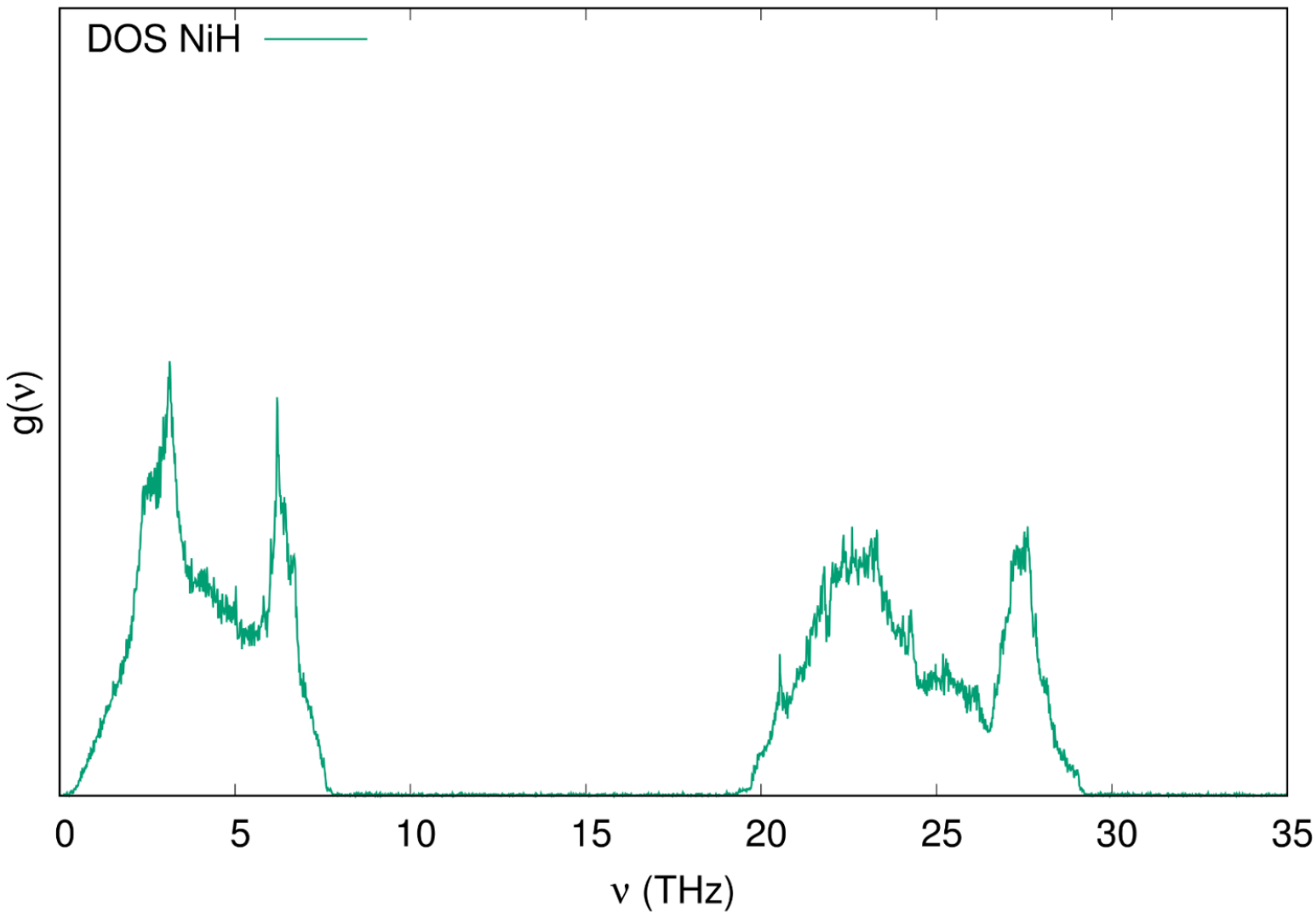

1 H atom (100) in NiH at T=0K

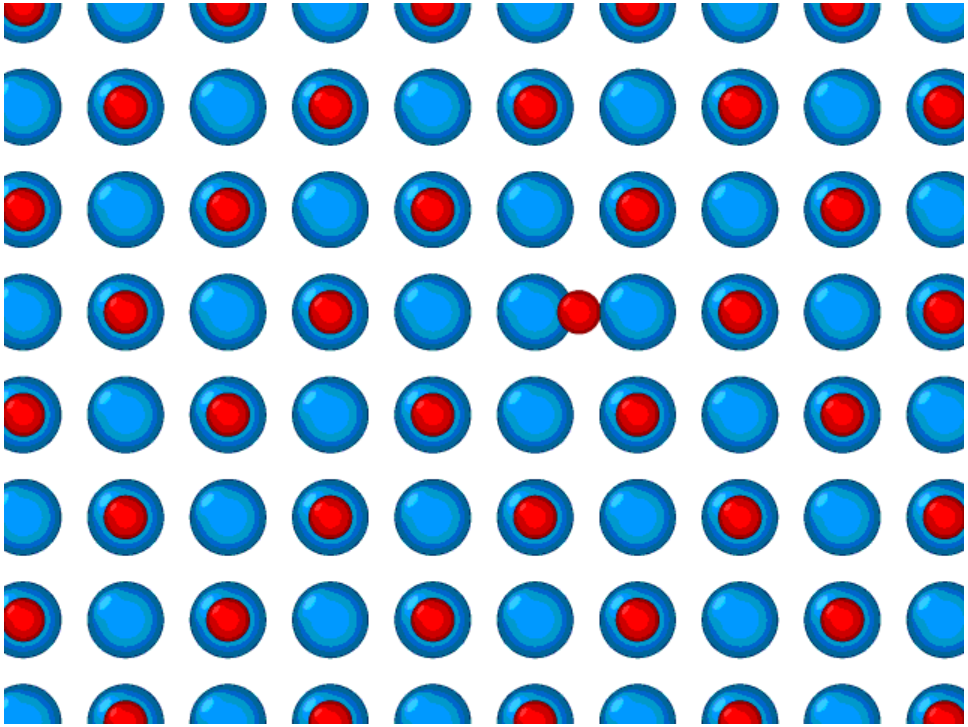

1 H atom (100) in NiH at T=0K

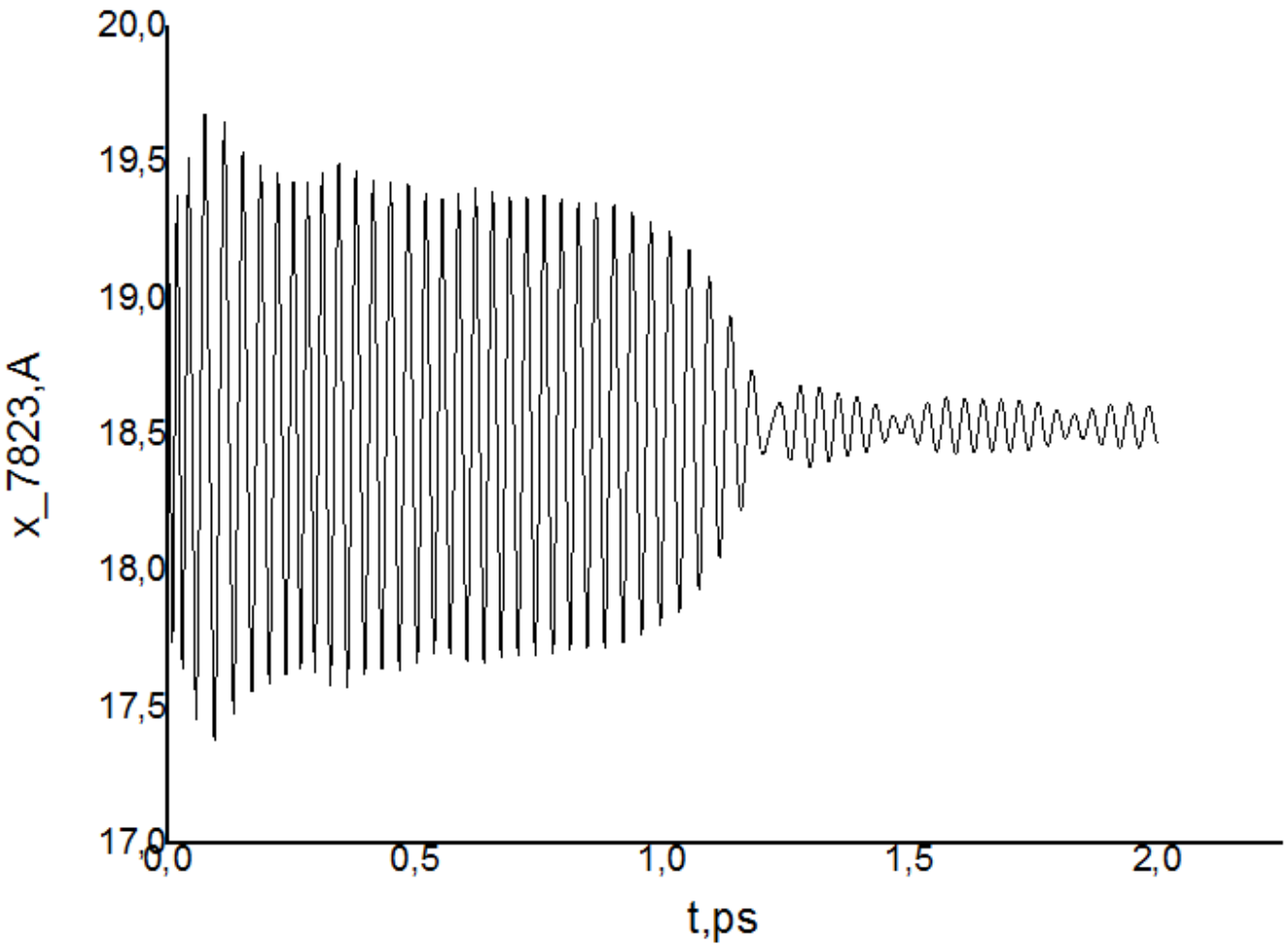

2 H atoms (100) and (-100) in NiH at T=0K

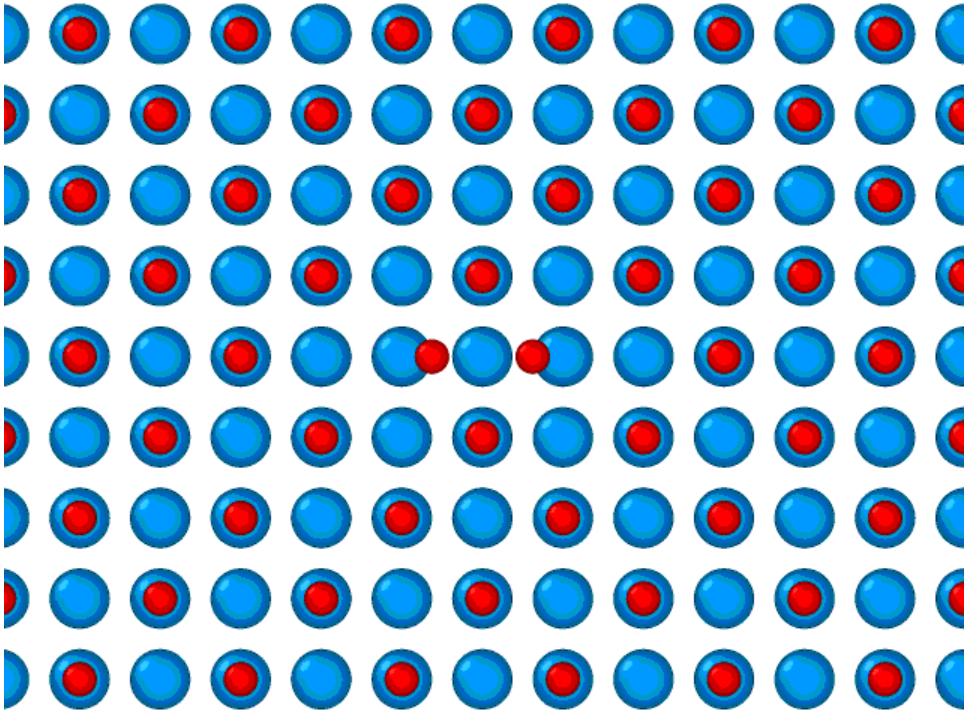

2 H atoms (100) and (-100) in NiH at T=0K

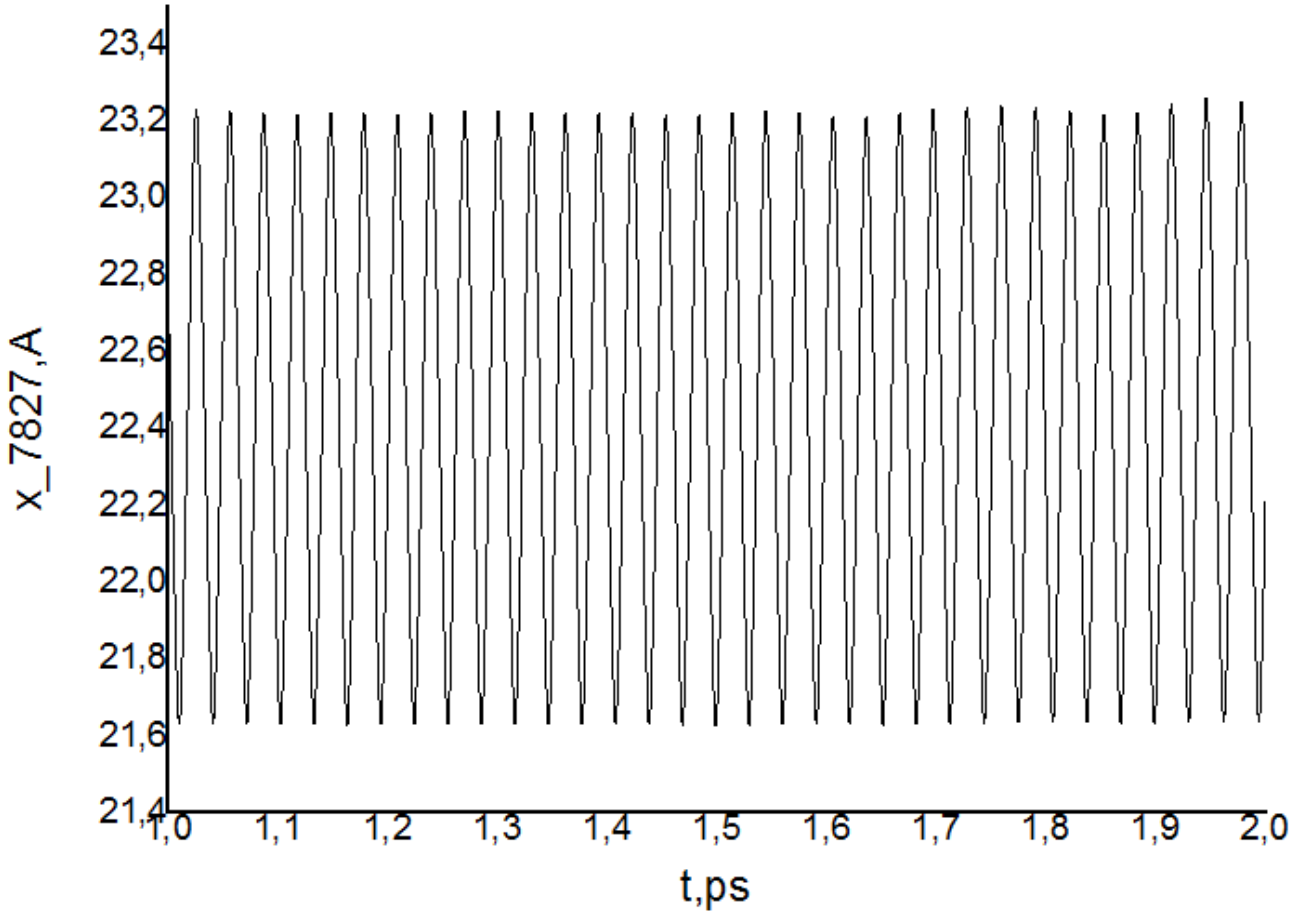

2 H atoms (100) and (-100) in NiH at T=0K

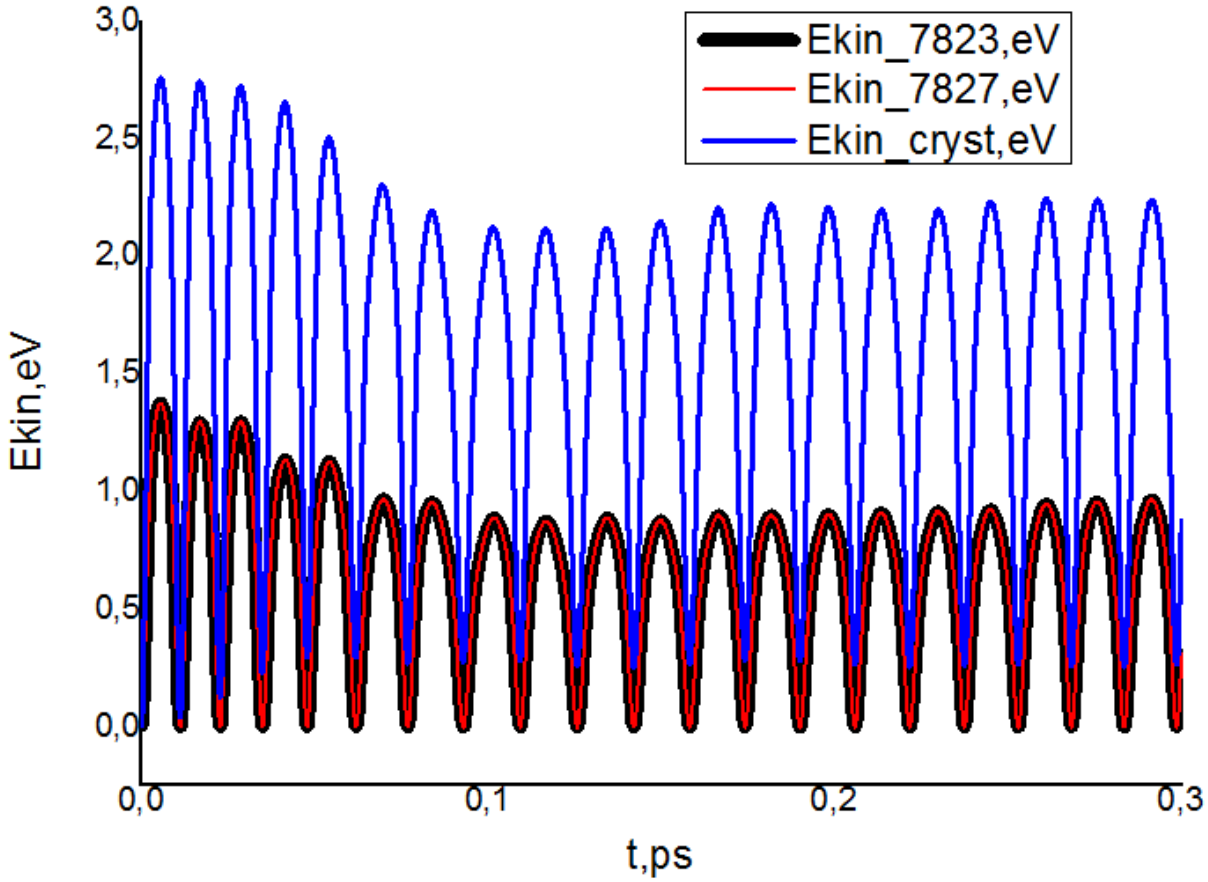

2 H atoms (100) and (-100) in NiH at T=0K

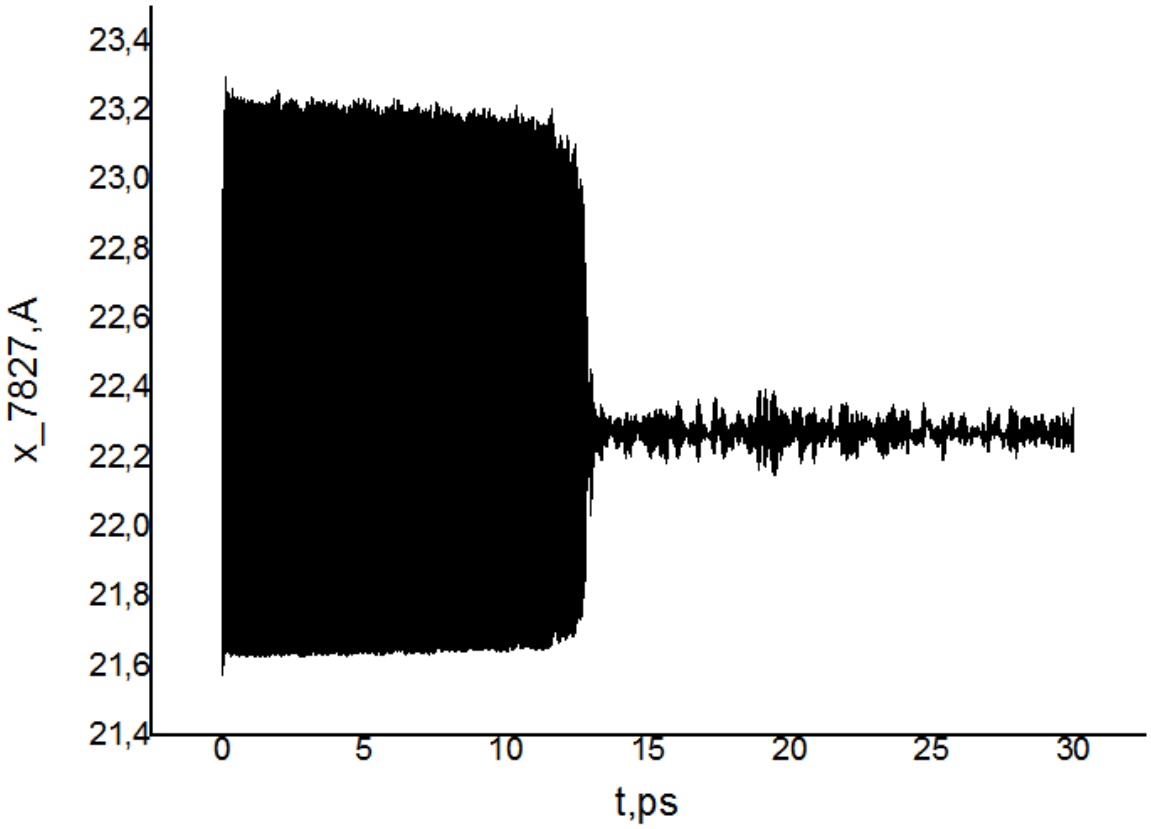

Visualization of the PdH fcc Lattice Oscillations at T=100 K

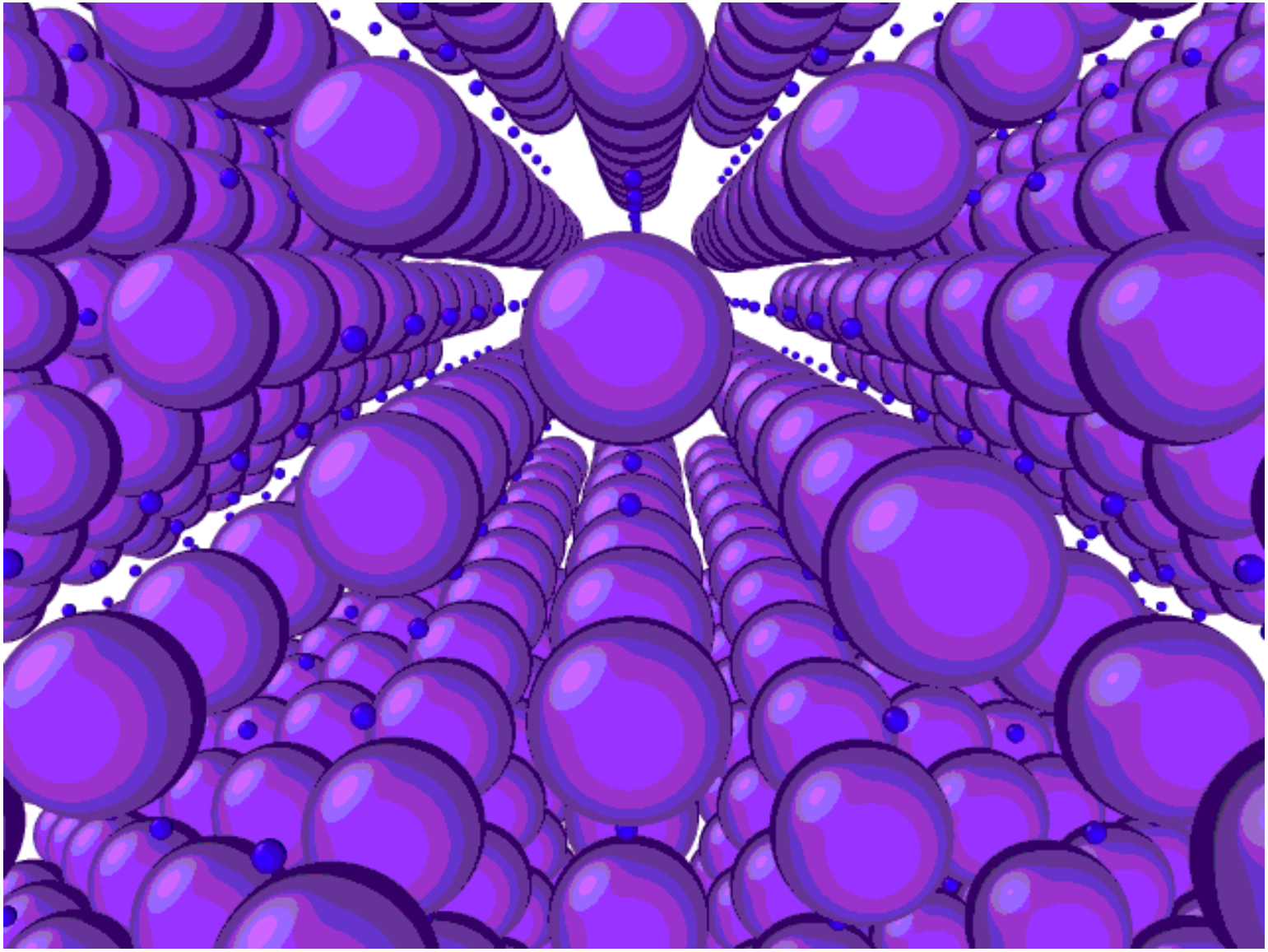

Visualization of the PdH fcc Lattice Oscillations at T=1000K

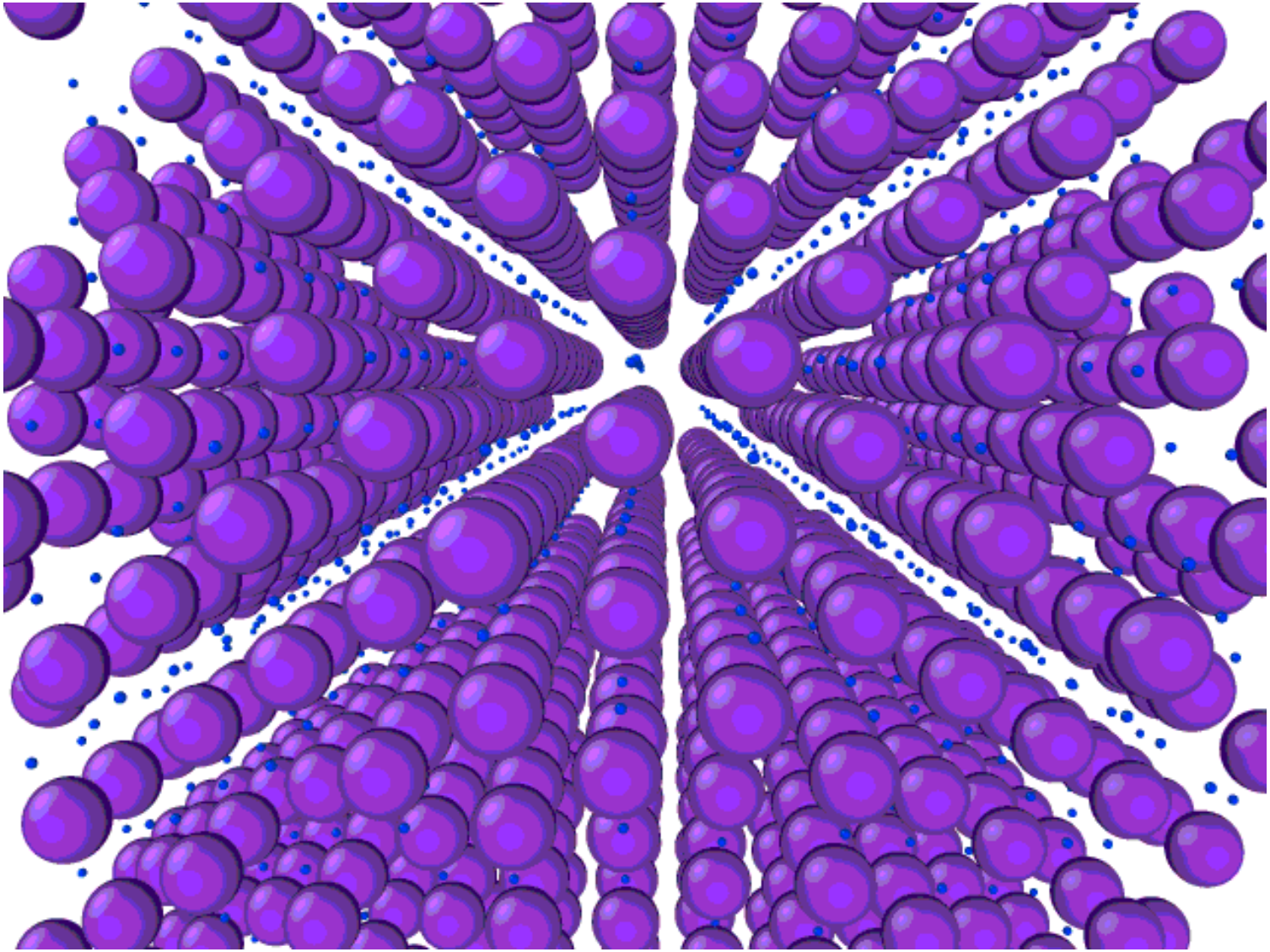

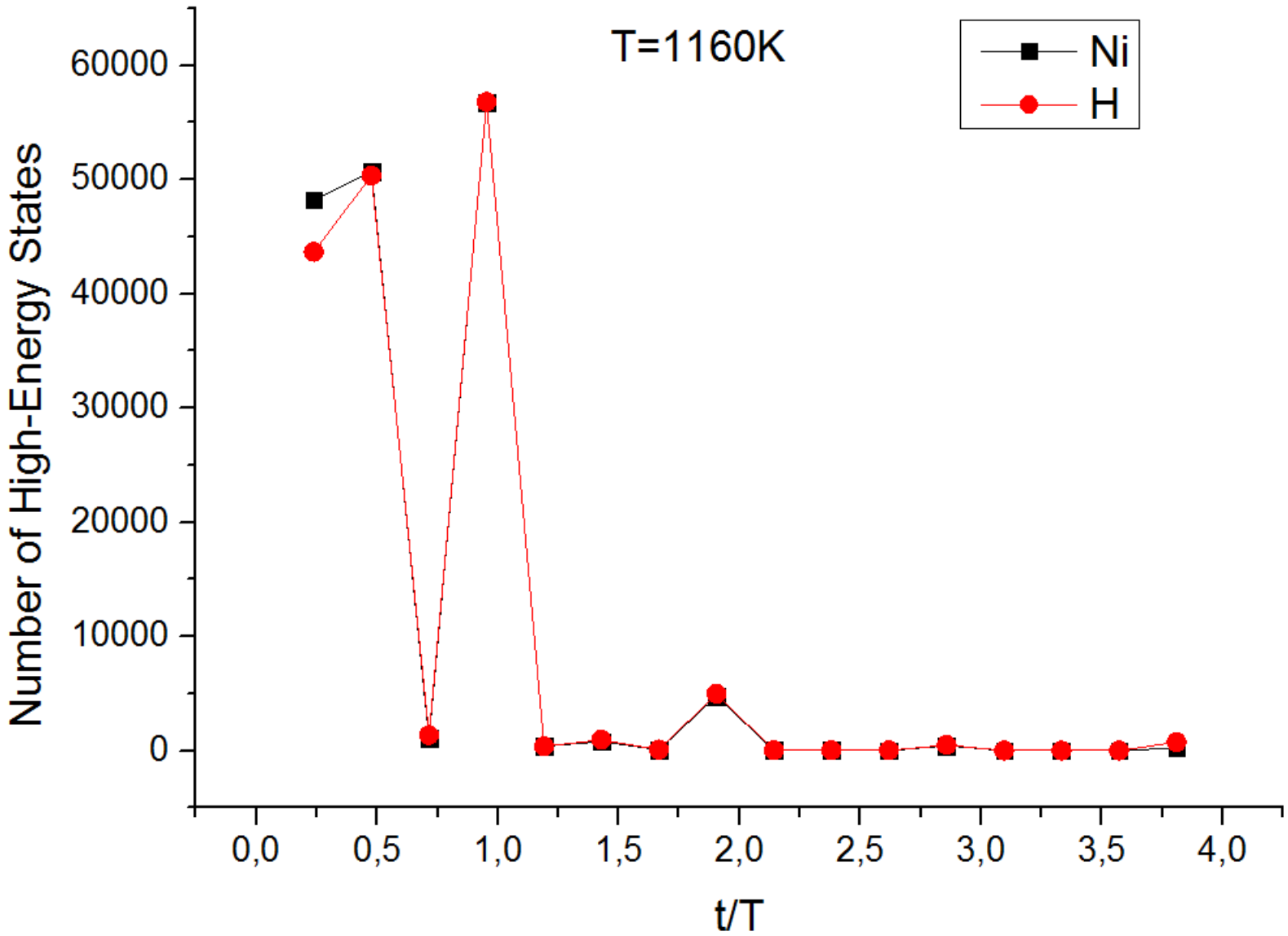
T=1160K
Ni
H
Number of High-Energy States
60000
50000
40000
30000
20000
10000
0
0,0
0,5
1,0
1,5
2,0
2,5
3,0
3,5
4,0
t/T

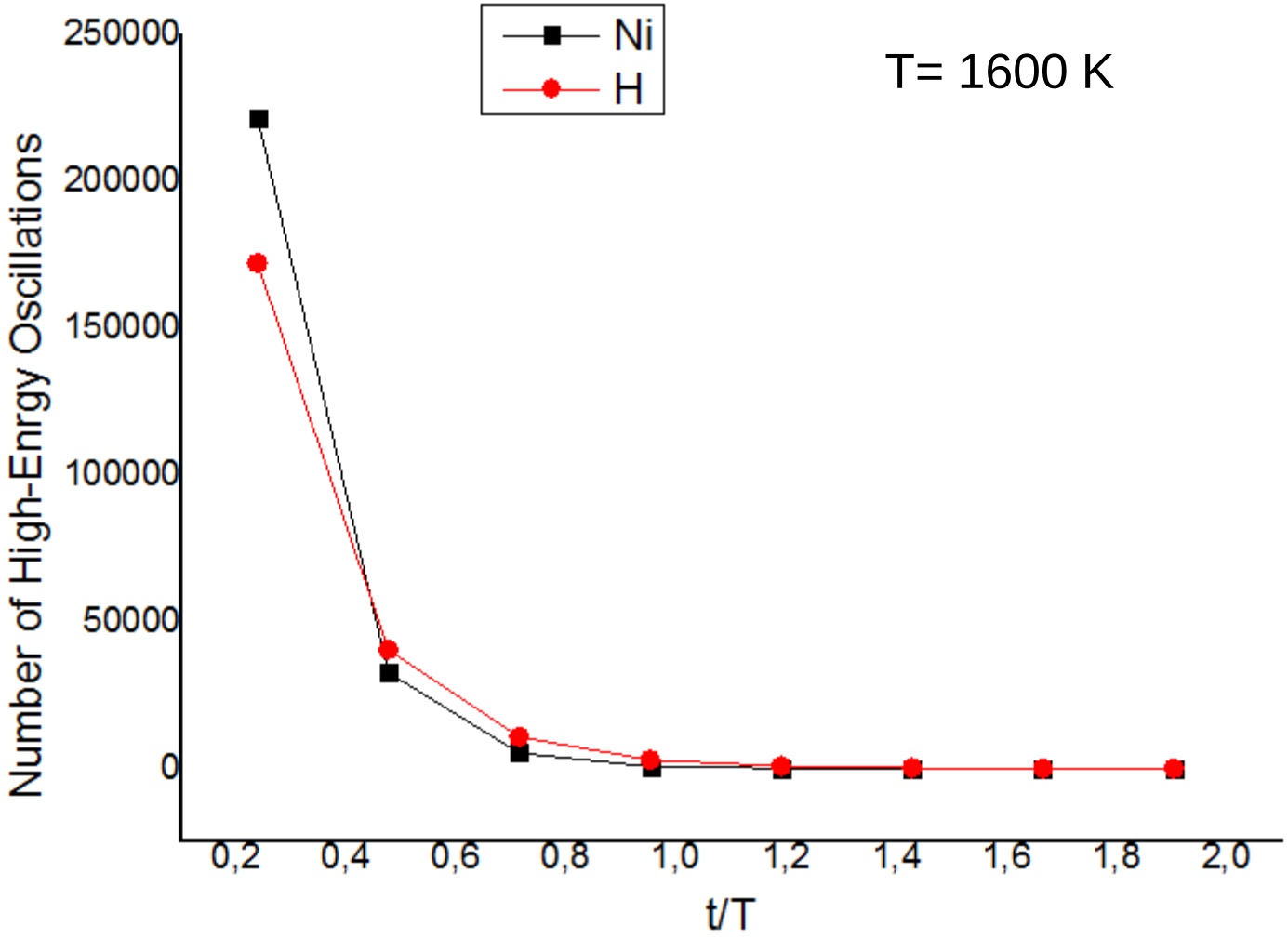
Ni
H
T= 1600 K
Number of High-Enrgy Oscillations
250000
200000
150000
100000
50000
0
0,2
0,4
0,6
0,8
1,0
1,2
1,4
1,6
1,8
2,0
t/T

Nickel nanoparticles, Zhang and Douglas (2013)

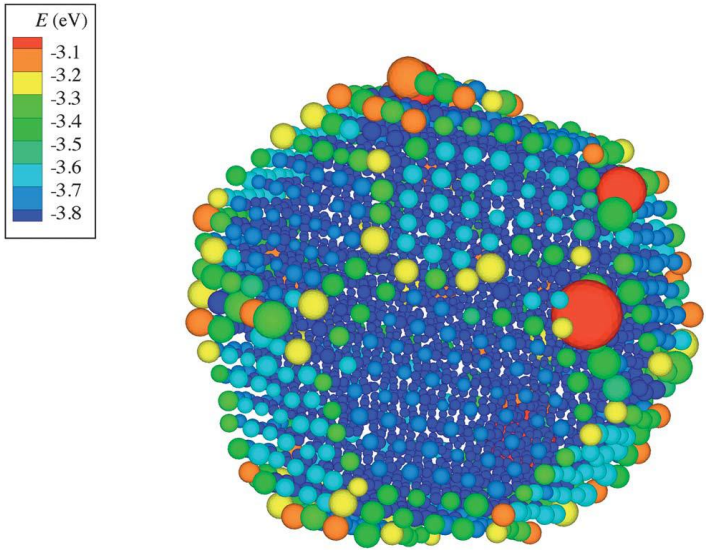

Atomic configuration of a Ni nanoparticle of 2899 atoms at T = 1000 K. The atoms are colored based on the potential energy and their size is proportional to Debye–Waller factor. Potential energy and DWF are time averaged over a 130 ps time window, corresponding to the time interval during which the strings show maximum length.

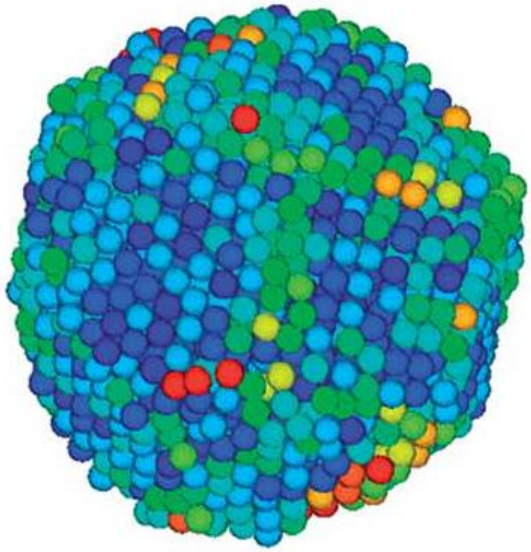

Map of the local Debye–Waller factor showing the heterogeneity of the atomic mobility at a temperature of 1450 K. Regions of high mobility string-like motion are concentrated in filamentary grain boundary like domains that separate regions having relatively strong short-range order.

Pd nanoparticles, Dubinko, Laptev, Terentyev (2017)

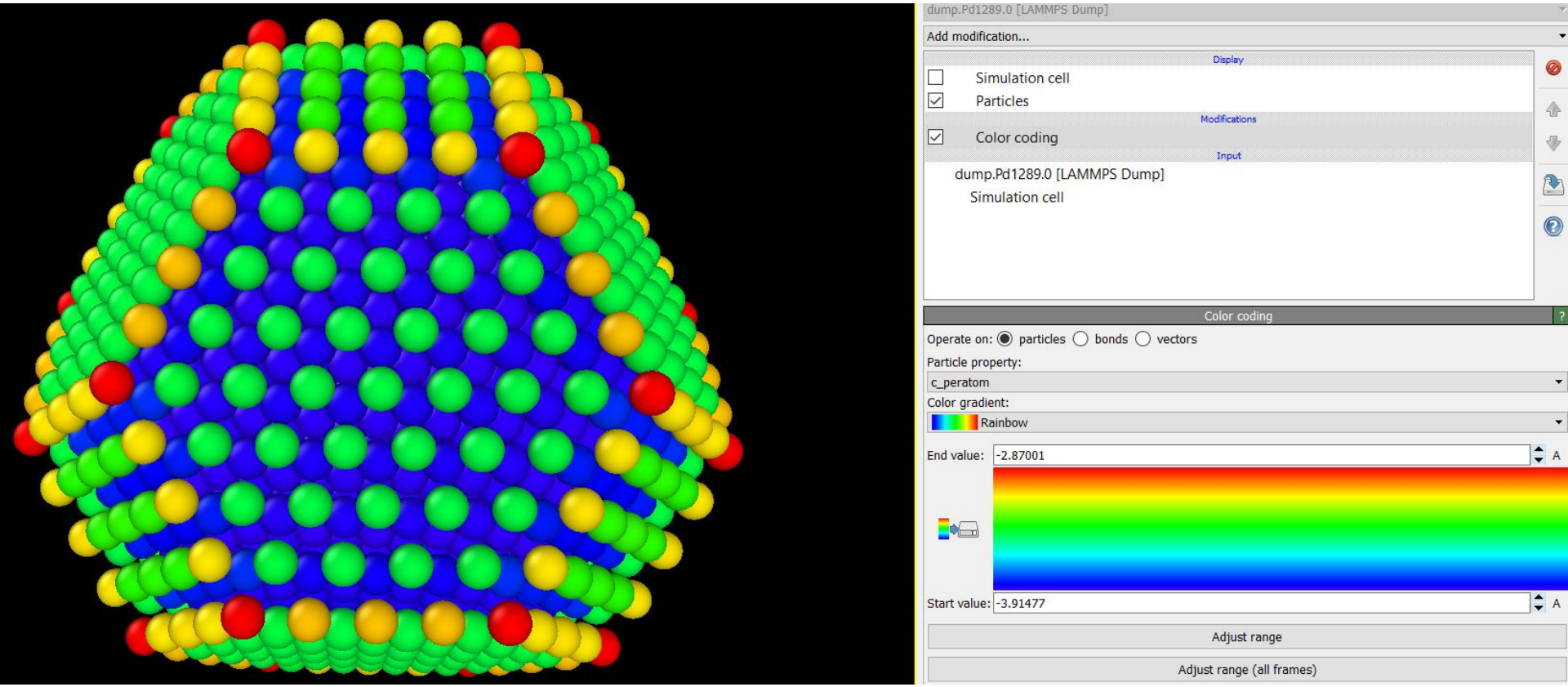

Epot_Pd_1289atoms_250K_d=3.1nm

Pd nanoparticles, Dubinko, Laptev, Terentyev (2017)

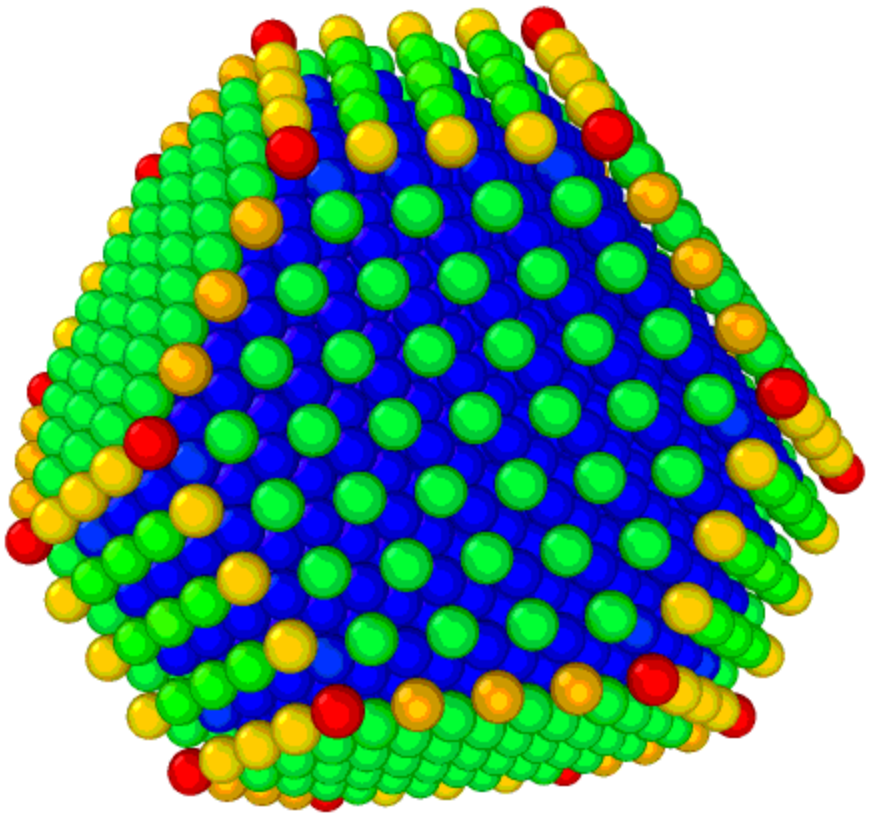

Epot_Pd_1289atoms_250K_d=3.1nm

Pd nanoparticles, Dubinko, Laptev, Terentyev (2017)

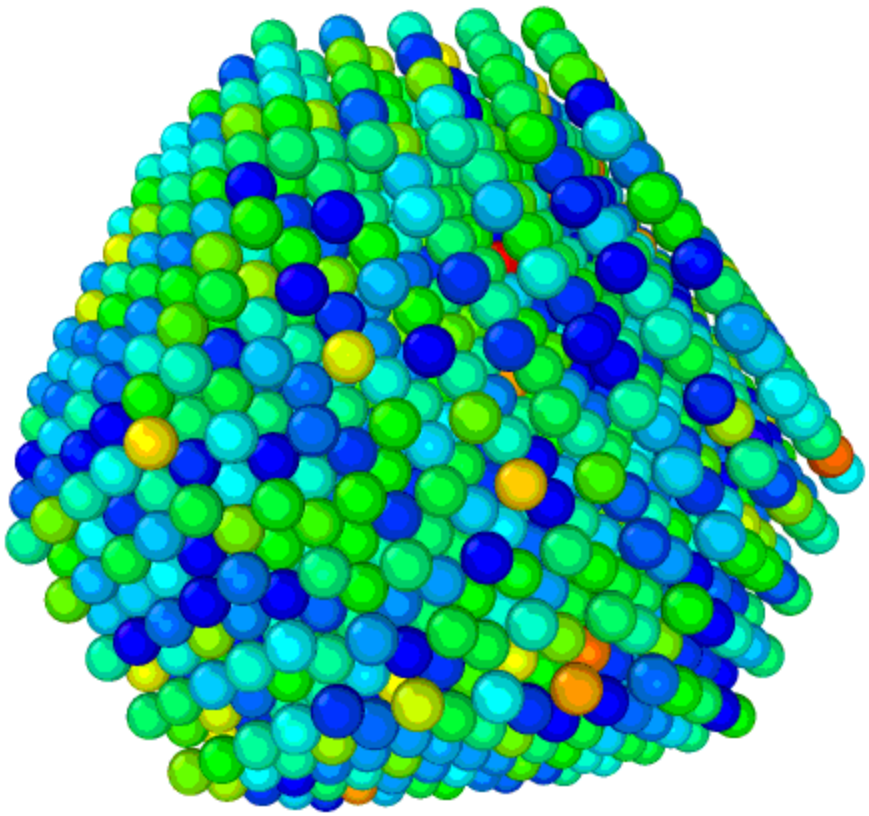

Ekin_Pd_1289atoms_250K_d=3.1nm

Magic Clusters

magic clusters (rus. кластеры, магические) — clusters of certain ("magic") sizes, which, due to their specific structure, have higher stability as compared to clusters of other sizes.

Number of atoms in the icosahedral cluster

$$n = (2N+1) + 10\sum_{k=1}^{N} k^2$$

$$n = 13, 55, 147, 309, 561$$

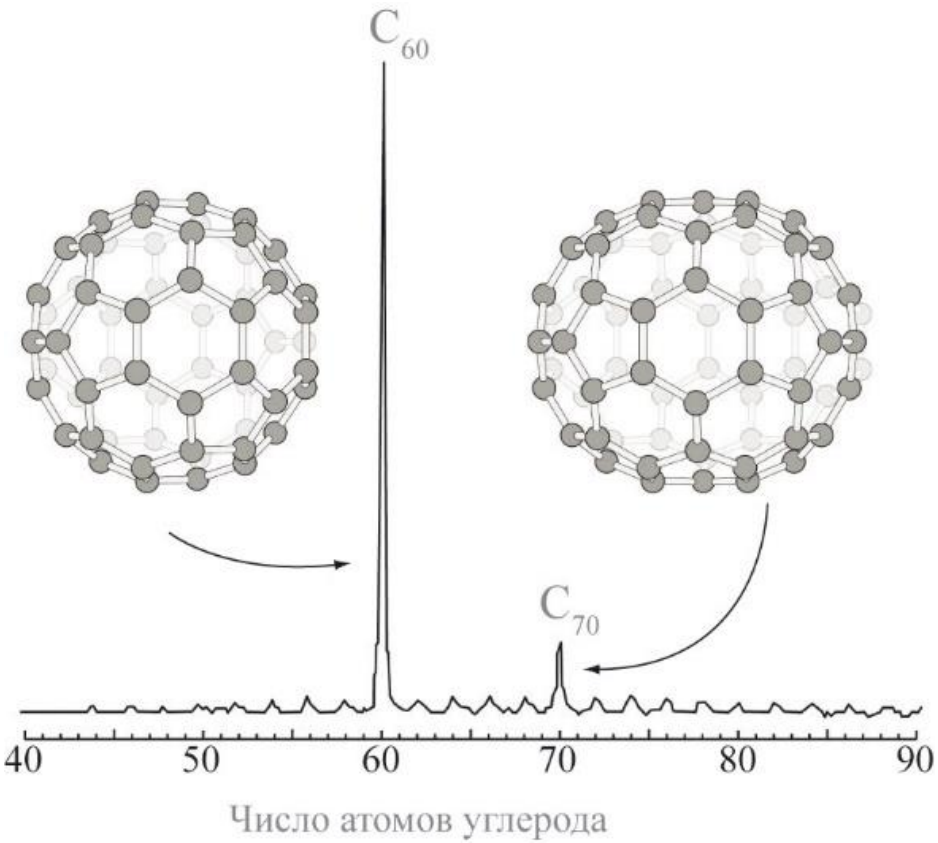

Mass spectrum of carbon clusters produced by laser evaporation of graphite. The highest peak corresponds to C_{60} fullerene molecules, and the less intensive peak represents C_{70} molecules

Quasi-crystaline Pd cluster

E0=0.1eV

Consider a cluster of 13 Pd atoms with quasi-crystalline 5th order symmetry axis.

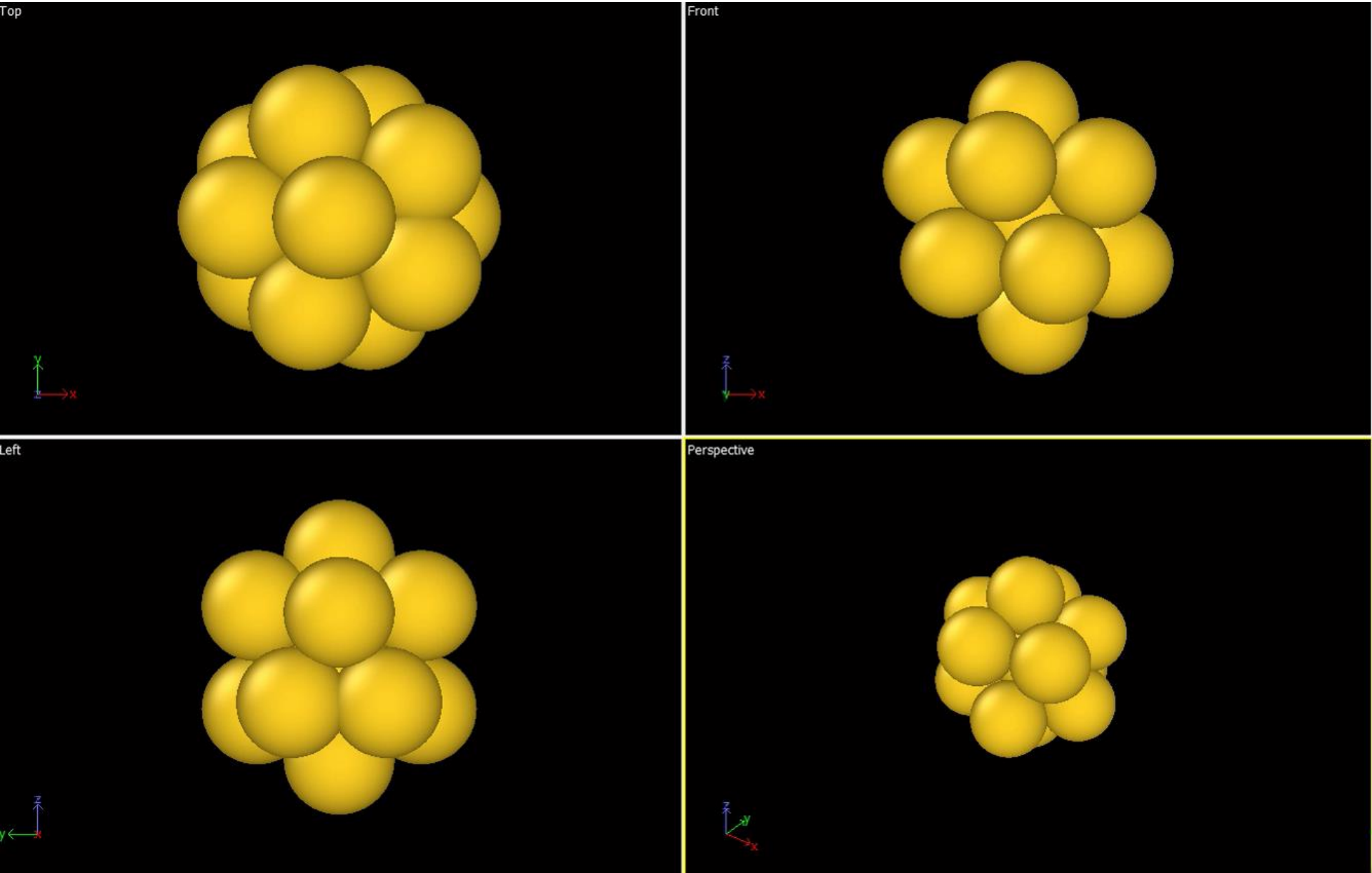

Magic icosahedral cluster of 55 Pd atoms

Consider a cluster of 55 Pd atoms with quasicrystalline 5th order symmetry axis.

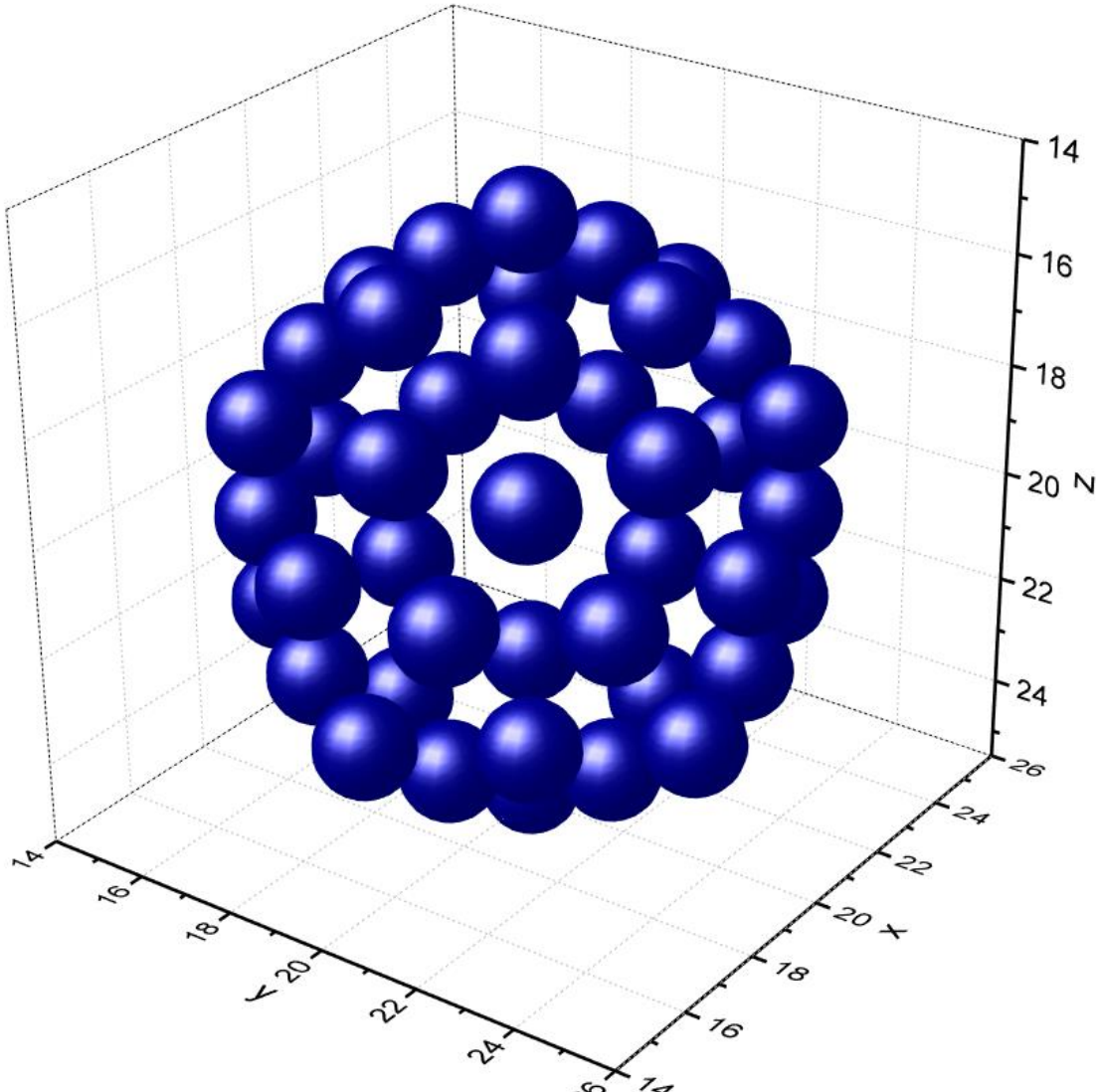

Icosahedral cluster of 55 Pd atoms

Initial conditions: at the initial time moment all particles have zero displacements from equilibrium positions.

Atom #1 has initial kinetic energy **1.5**eV in [00-1] direction.

Atom #12 has initial kinetic energy **1.5**eV in [001] direction

Boundary conditions: free surfaces of cluster

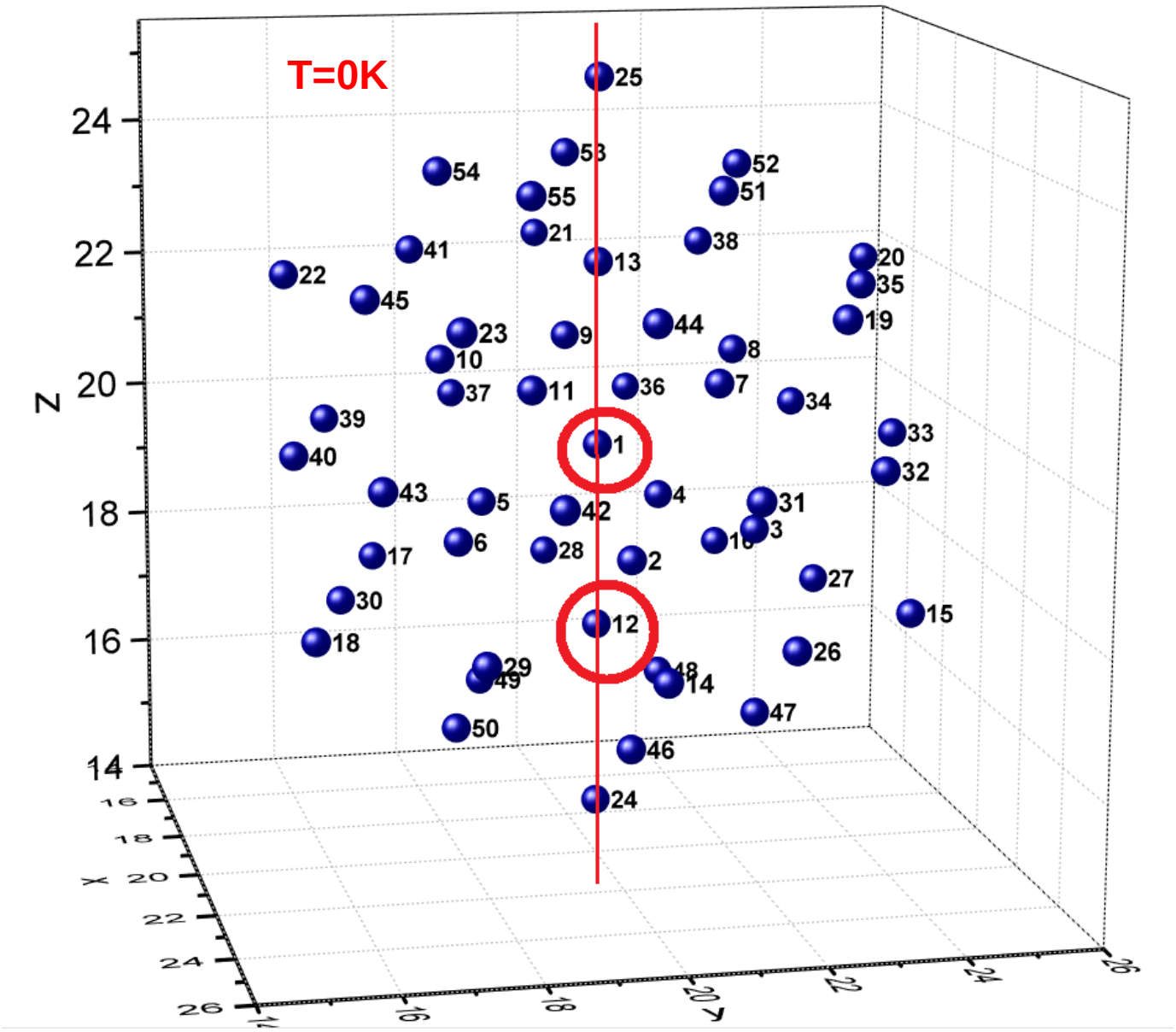

Dynamics of the icosahedral cluster of 55 Pd atoms

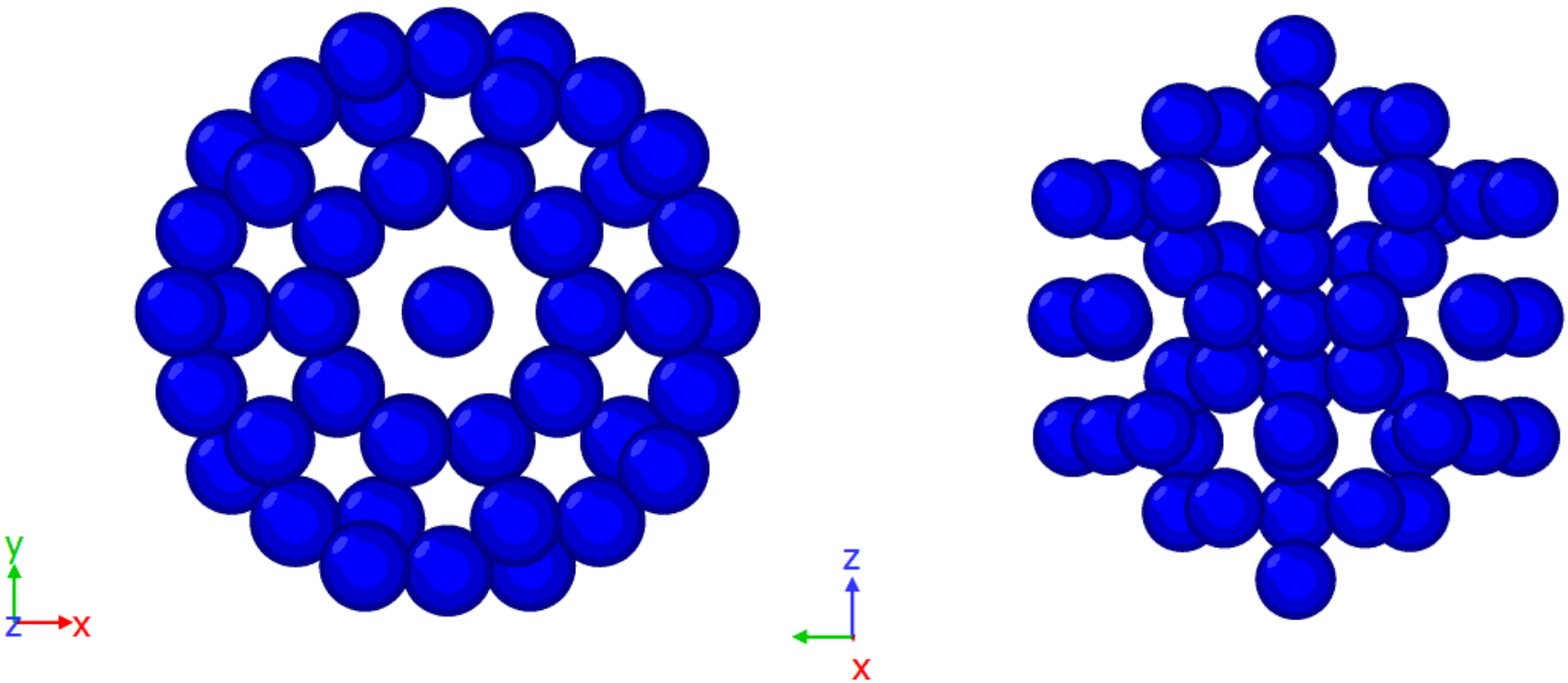

It is seen from the visualization, that Localized Anharmonic Vibration is generated. The observed LAV in the atomic cluster represents the coherent collective oscillations of Pd atoms along quasi-crystalline symmetry directions.

Dynamics of the Pd atomic cluster

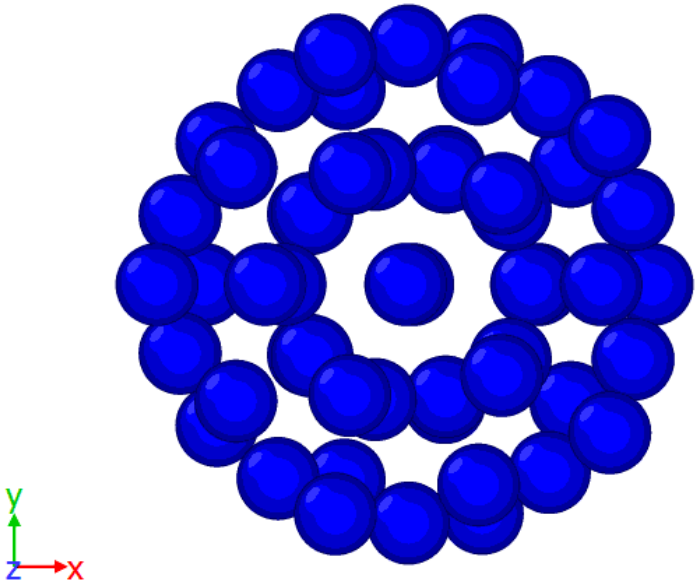

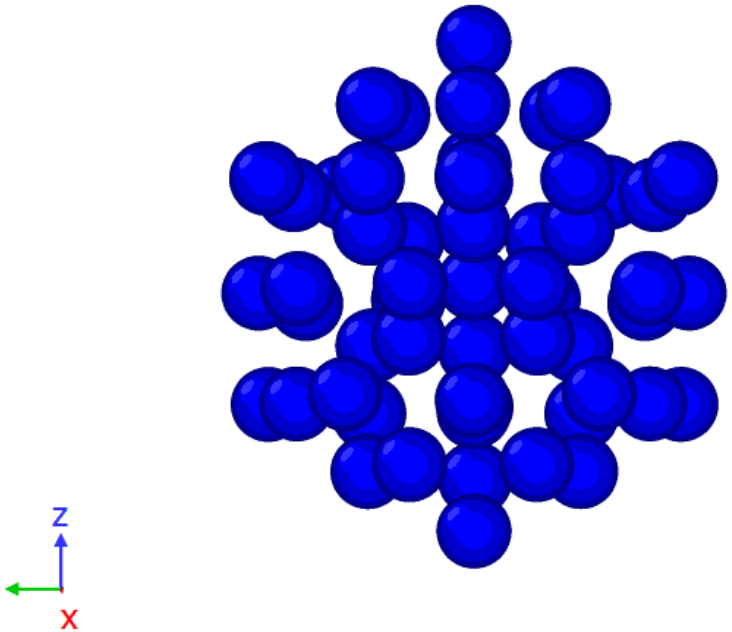

If the initial energy, given to cluster is large enough (greater then the cohesive energy) then the cluster is destroyed after a certain period of time (~ ps) .

Conclusions and outlook

New mechanism of chemical and nuclear catalysis in solids is proposed, based on **time-periodic driving** of the potential landscape induced by *emerging nonlinear phenomena*, such as LAVs.

The model (*under selected set of material parameters*) describes the reported exponential dependence on temperature and linear dependence on the electric (or ion) current.

Atomistic modeling of LAVs in metal hydrides/deuterides may offer ways of ***engineering the nuclear active environment*** .

Outstanding problems:

Existence and properties of LAV at elevated temperatures

Account of quantum effects in MD/DFT at low temperatures

Experimental verification of LENR

Publications

1. V.I. Dubinko, P.A. Selyshchev and F.R. Archilla, *Reaction-rate theory with account of the crystal anharmonicity*, **Phys. Rev**. **E** 83 (2011**),**041124-1-13
2. V.I. Dubinko, F. Piazza, *On the role of disorder in catalysis driven by discrete breathers*, **Letters on Materials** 4 (2014) 273-278.
3. V.I. Dubinko, *Low-energy Nuclear Reactions Driven by Discrete Breathers*, **J. Condensed Matter Nucl. Sci**., 14, (2014) 87-107.
4. V.I. Dubinko, *Quantum tunneling in gap discrete breathers*, **Letters on Materials**, 5 (2015) 97-104.
5. V.I. Dubinko, *Quantum Tunneling in Breather 'Nano-colliders'*, **J. Condensed Matter Nucl. Sci.**, 19, (2016) 1-12.
6. V. I. Dubinko, D. V. Laptev, *Chemical and nuclear catalysis driven by localized anharmonic vibrations*, **Letters on Materials** 6 (2016) 16–21.
7. V. I. Dubinko, *Radiation-induced catalysis of low energy nuclear reactions in solids***,** **J. Micromechanics and Molecular Physics**, 1 (2016) 165006 -1-12.
8. V.I. Dubinko, O.M. Bovda, O.E. Dmitrenko, V.M. Borysenko, I.V. Kolodiy, *Peculiarities of hydrogen absorption by melt spun amorphous alloys* $Nd_{90}Fe_{10}$*, Vestink KhNU (2016).*
9. V. Dubinko, D. Laptev, K. Irwin*, Catalytic mechanism of LENR in quasicrystals based on localized anharmonic vibrations and phasons,* **ICCF20***,* https://arxiv.org/abs/1609.06625. to be published in **J. Cond. Matter Nucl. Sci**

Acknowledgments:

- The authors would like to thank Dmitry Terentyev for his assistance in MD simulations
- Financial support from Quantum Gravity Research is gratefully acknowledged.

THANK YOU
FOR YOUR ATTENTION!